NTNU
Norwegian University of
Science and Technology

Immobilisation of *E. coli* by Microarray Printing.

Retina Shrestha

MSc in Biology
Submission date: June 2018
Supervisor: Marit Sletmoen, IBT

Norwegian University of Science and Technology
Department of Biotechnology and Food Science

Abstract

Cellular heterogeneity is a fundamental property of organisms that help them to adapt and thrive in different changing environmental conditions. Therefore, approaches are necessary to study cellular processes at a single cell resolution. One of the rapidly evolving technologies is microcontact printing (μCP) which is a simple, fast, cost-effective and reliable method for preparation of microarrays. Bacterial microarrays are used to deposit bacteria on a solid substrate in regular and well-defined positions. They are used to study variations of bacterial cells and their responses are also analysed. Currently, atomic force microscopy(AFM) is widely used for cellular studies of different bacteria by measuring the forces driving cell-cell and cell-substrate interactions on a single cell basis.

The thesis work was focused on immobilisation of *E. coli* cells by microarray imprinting. To achieve this, PDMS stamps with circular spots of different diameters were prepared. Chemicals known to support bacterial attachment like poly-L-lysine (PLL), mannan and polydopamine (PD) were applied on top of PDMS stamps and deposited on PEGylated glass surfaces. *E. coli* cells were added to the patterned surfaces.

The micro-contact printing of PLL-FITC was successful on both clean and PEGylated glass surfaces. *E. coli* cells were successfully immobilised on PEGylated glass surfaces with PLL spots whereas mannan and PD spots on PEGylated glass surfaces did not produce strong immobilisation of *E. coli* cells. The obtained results demonstrated that it is possible to deposit *E. coli* cells on PEGylated glass surfaces on PLL spots. Further, AFM analysis showed that there is a higher interaction between *E. coli* and aminated mannan-coated surfaces as compared to *E. coli* and clean glass surfaces.

Acknowledgement

The work presented in this master's thesis was performed at the Department of Biotechnology and food science at the Norwegian University of Science and Technology (NTNU). Some experimental works were carried out at NTNU Nanolab.

I would like to extend my sincere gratitude to my thesis supervisor Marit Sletmoen for her continuous support with optimistic attitude, constructive feedbacks, motivations and directions throughout the project.

My special thanks to post-doctoral fellows Swapnil Bhujbal and Alex Wong for their guidance and providing me with *E. coli* cells and growth medium for the experiments.

I am thankful to the staffs at Nanolab for their advice through out my research. Moreover, I also extend gratitude to my fellow master's students and PhD fellow Karen Dunker for their valuable assistance whenever I needed.

To end with, I would like to thank my family, my boyfriend and friends for their continuous love, support and encouragement during the project.

Table of Contents

List of Figures

Abbreviations

AFM	Atomic force microscopy
BSA	Bovine serum albumin
cDNAs	Complementary deoxyribose nucleic acid
CH3	Methyl
CF3	Trifluoromethyl
DNA	Deoxyribose nucleic acid
DUV	Deep ultra violet
E. coli	*Escherichia coli*
EDC	N-(3- Dimethylaminopropyl)-N' ethyl carbodiimide hydrochloride
EPEC	Enteropathogenic *Escherichia coli*
FD	Force-distance
FITC	Fluorescein isothiocyanate
HCL	Hydrochloric acid
HEPES	(4-(2-hydroxyethyl)-1-piperazineethanesulfonic acid
IPA	Isopropyl alcohol
LB	Lysogenic broth
LbL	Layer by layer
LOC	laboratory-on-a-chip
LPS	Lipopolysachharide
kDa	kilodaltons
M	Molar [mol/L]
Mw	Molecular weight
MAP	Mussel adhesive protein
MPa	Megapascals
MQ	Milli Q
MS	Mass Spectrometry
NMR	Nuclear magnetic resonance
NA	Numerical aperturer
NaCl	Sodium chloride
NTNU	Norwegian University of Science and Technology
N_2	Nitrogen
PBS	Phosphate buffered saline
PD	Polydopamine
PDMS	Polydimethylsiloxane
PEG	Poly (ethylene glycol)
PEI	Polyethylenimine
Pic(BH3)	Picoline borane
PLL	Poly-L-Lysine
PVA	Polyvinyl alcohol
Rpm	Rotations per minute
SAM	Self-assembled monolayer
SYTO 9	Cytochrome 9
TRIS	Tris(hydroxymethyl)aminomethane
UPEC	Uropathogenic *Escherichia coli*
UV	Ultra violet

UTI	Urinary tract infection
Λ	Wavelength
μCP	Microcontact printing

1 Introduction

The discovery of cell through the invention of the single lens microscopy by Antonie van Leeuwenhoek in the late 1600s paved the path for current advancement in cytology. Improvement in microscopy like powerful microscope lens, and better staining techniques have allowed the study of key components of cells including the cell surface and sub-cellular organelles [1]. After the discovery of cells, various improvements have been made in the field of cellular and molecular biology. The discovery of the structure of DNA stands out as the dawn of the molecular genetics followed by the establishment of the central dogma and solving the genetic code [2]. Subsequent development in the field of biology like nucleic acid and protein sequencing led to the initiation of an 'omics' era beginning with genomics followed by proteomics, transcriptomics and metabolomics. Further, the development of systems biology and bioinformatics tools enabled the systematic study of complex interactions of structure and function in biological systems. Recently most of these 'omics' studies are focused at the single cell level. The concept of single cell analysis stems from the fact that a cellular population is heterogeneous and each cell can have distinct genotypic and phenotypic characteristics [3].

Heterogeneity between each cell might be a vital part of the cellular processes like signalling, transcription, and other cell fate [4]. The bulk measurement of cellular heterogeneity produces ensemble averages, which not only prevent the study of fine structures and block identification of rare cells but also the gene expression of individual cells, is masked by the dominant cell type [5]. Therefore, by analysing single cell, underlying mechanisms of cellular heterogeneity can be known [3]. This recent development of single cell analysis has aided detailed and comprehensive studies of individual cells [6].

1.1 Aim of the thesis

- To produce PDMS stamps with micrometer features.
- To develop cheap, easy and reliable methods of microcontact printing to deposit chemicals like mannan, PLL, and polydopamine.
- To I mmobilize *E. coli* on the microcontact printed pattern with these chemicals.

2 Background

A single cell is made up of various molecular constituents making it a complex system [7]. The heterogeneity between different cells is an essential characteristic of cellular populations, and it can be either genetic or phenotypic. The genetic heterogeneity arises due to the presence of subpopulations with a typical phenotype and various DNA sequences caused by mutation, whereas the phenotypic heterogeneity designates morphological variation within a cellular population without any genotypic differences [8]. Stochastic variations or noise in gene expression of isogenic cells is considered as the principal molecular cause of this phenotypic heterogeneity [9]. It is known that numerous bacterial populations survive and adapt to changing environments by exhibiting phenotypic heterogeneity [10]. One of the most common phenotypic heterogeneity is bacterial persistence, whereby isogenic bacterial populations can thrive antibiotic treatment without being resistant to the antibiotic [11].

Most of the methods to study bacterial and other microbial cell populations provide population averages. These population averages of a large number of homogenized cells can produce misleading mean values, which mask small but critical changes within individual cells resulting in loss of information related to transcriptional variability of individual cells as well as the relationship between specific genes in single cells. Thus, these approaches are not suitable to study cellular heterogeneity and complexity of tissues [12].

Single cell analysis permits the study of cell-to-cell variation of different organs, tissues, and cell cultures [13]. In simpler form, it reduces biological noise [5]. Recent investigations use fluorescent proteins like green fluorescent proteins combined with fluorescence microscopy or flow cytometry to study single cell. In flow cytometry, heterogeneous mixture of cells is passed through a laser light beam in a single file fashion. Different components of the cell are tagged with fluorescence molecules which emit light at various wavelength. This emitted light is correlated with different physical and chemical characteristics of cells. However, this method does not track a cell over time [14]. Microarrays with high throughput analysis and miniaturization help to study various biomolecules such as proteins, DNA, and living cells. DNA microarrays help for genomic studies whereas protein microarrays are used for proteomic studies [15]. Transfected cell microarrays represent a complementary technique in which array features have clusters of cells overexpressing defined cDNAs [16].

One of the recent and rapid developments in micro- and nanofabrication technologies for single cell analysis is the ‘laboratory-on-a-chip’ (LOC) An exceptionally precise microprinted method

has also been developed for this purpose [13]. The microprinted method generally includes patterning of surfaces for cellular adhesion for single cell analysis. This method helps to create surface patches onto which cells are likely to attach contrasted by cell-repellent areas on the substrate surface [17].

However, there is still an absence of an appropriate microprinted approach to study the most common bacteria (e.g., *E. coli*), which may be due to their small size (1-5 µm) and motility [18]. So, this project is dedicated to finding the methods for developing microcontact printing as a potential technique for single cell isolation using *E. coli* as a model organism.

3 Theoretical background for the methods used

3.1 Photolithography

Photolithography forms or degrades a polymer network in a specific geometric pattern on a substrate by using light, and a photomask. The substrate can be glass but most commonly a 2-4 inch diameter silicon wafer is used. A photoresist is a mixture of organic polymer that is sensitive to light of a certain wavelength and changes its chemical structure when exposed to UV light. A photosensitive polymer that is deposited on the wafer is selectively degraded to produce a patterned substrate. There are two different photoresists: positive and negative. An insoluble polymer of a positive photoresist becomes soluble when it is exposed to UV light. A negative photoresist polymerizes to form insoluble polymers upon UV exposure and the developer solution removes only the unexposed areas [19]. A photomask, made up of quartz or glass, is an opaque plate with holes or transparencies that lets light pass through predetermined areas to project an image on a surface [20]. Photolithography is widely used in the semiconductor industry for manufacturing integrated circuits and other digital media [19].

Brief procedure for the photolithography

The silicon wafer is first cleaned with organic solvents to remove particulate matter that can cause the irregular thickness of the photoresist along with holes and cracks on it. Afterwards, it is subjected to oxygen plasma treatment to increase the surface wettability and remove impurities on the surface. A dehydration bake is then performed to evaporate any remaining water and improve resist adhesion to the wafer. Then a thin uniform layer of photoresist is applied on the substrate surface by spin coating. The thickness of the resist layer is adjusted by changing the parameters like the speed, angular acceleration and angular viscosity of the photoresist. The next step is the soft bake, where the wafer is heated on a hot plate for a specified and resist-dependent time and temperature. This process helps to remove all the solvents from the photoresist coating without degradation of its components increasing the thickness of the layer and prepare the photoresist to be exposed to the UV. Soft baking is essential for photo-imaging as it makes the photoresist coatings photosensitive or imageable. In case of positive photoresists, it's cross-linking, or polymerization process hardens the layer. These cross-links are photochemically unstable and are broken if exposed to UV lights of a manufacturer-specified wavelength [21].

The substrate is then exposed to UV light through the photomask for a set amount of time. The exposed areas are removed when washed in a developer solution whereas the unexposed

substrate remains. Therefore, the pattern formed on the wafer is an exact copy of the pattern present on the mask. Many resist also require a second baking step, referred to as the post-exposure bake, after exposing to UV. The temperature and duration of the post-exposure bake have been found to be a critical step in the photolithography process. After the post-exposure bake, the wafer is placed in a developer solution that dissolves determined areas of the resist to reveal the designed pattern. The finished master mould can then be used for further processes, such as replica moulding with PDMS [22].

3.2 Microcontact printing (μCP)

In the early 1990s, Kumar and Whitesides used a micro-structured elastomeric stamp to develop μCP for the patterned transfer of thiols onto gold surfaces. Since then, it has been used in different fields to pattern water, salt, organic solvents, metals, polymers, DNA, proteins, and cells [23]. Moreover, in the fields of chemistry and biology, μCP is applicable in forming micropatterns for drug and cellular measurement [24].

μCP is an advanced form of simple stamping process that involves ink, stamp and substrate. The major substance is a flexible elastomeric stamp, with microscopic patterned relief structures on one of the side of its surface, which is produced by soft lithography approaches. The ink solution is a chemical reactant commonly made up of proteins, protein mixtures or small molecules. Frequently utilized substrate for μCP are glasses, silicon or ultra -flat metal [25]. The process has been used to pattern molecules with micrometer and nanometer resolution and is demonstrated in figure 4.4. Microscale patterns of adhesive biomolecules, like collagen and fibronectin in cell-repellent substrates, have also been produced. This led to cellular arrays in which cell growth is prohibited to the islands of adhesive materials. Therefore, such patterning approaches can produce *in-vitro* culture of geometrically organized cell communities [24].

The μCP technique is easy to perform in a laboratory without continuous access to the cleanroom, and photolithographic equipment and the features can be printed efficiently in a single step. Besides, μCP uses elastomeric stamps that can adapt to the curved substrates as well. The μCP with 300 nm width has been optimized for the routine production [26]. The careful handling and planning of the stamping geometry can reduce the width of μCP to 30nm [27].

3.2.1 Principle of microcontact printing

Polydimethylsiloxane (PDMS)

The soft lithography is a non-photolithography method that uses elastomeric stamps to prepare micro/nanoscale patterns on different substrates like glass. PDMS is the most commonly used silicone elastomers for stamp preparation for µCP as it is cost-effective, and simple to produce. Several other elastomers like polyurethanes, polyamides, phenol formaldehyde polymer can also be used for patterning surfaces. PDMS has an inorganic siloxane backbone and two organic methyl groups attached to silicon as shown in figure 3.1. The PDMS stamps used for µCP is a two-component Sylgard 184 elastomer available from Dow Corning in the specified 1: 10 ratio of a catalyst or curing agent to prepolymer vinyl-terminated PDMS base. The curing agent is a mixture of a platinum complex and copolymers of methylhydrosiloxane and dimethylsiloxane. Increase in ratio of curing agent to base produces stiff PDMS stamp [28].

PDMS has numerous properties that make it suitable for µCP. It is a fluid prepolymer at room temperature due to its low melting point (about -50°C) and glass transition temperature (about -120°C), and it can be easily cured into solid by cross-linking. The polymer generally has Young's modulus around 1.5 MPa, which makes it flexible enough to form conformal contact with planar as well as nonplanar surfaces. It molds with very high fidelity to a patterned template Further, PDMS is transparent with the refractive index of 1.41 [25]. Besides, PDMS is highly elastomeric, due to which it deforms elastically not plastically over a wide range of strain. The elastomeric properties of PDMS are responsible for conformal contact of PDMS to substrate with little or no applied pressure. PDMS has low surface energy (22 dyne/cm^2) due to which it is easily released from the substrate after stamping [26]. The flexibility of the siloxane chain and the low intermolecular forces between the methyl groups are responsible for reducing the surface energy of PDMS. Further, fluorinated silanes can be bound to the template to lower the surface energy, which in turn enhance peeling off the stamp from the template. PDMS has inert surface and resists reaction with many chemicals, but it swells in organic solvents, that restricts its application in patterning chemicals dissolved in them. Larger features of pattern and smaller gaps between them was seen with swelling of the stamps in an organic solvent [28]. Furthermore, it is durable; the stamps can be used for more than 100 times [27]. It has modifiable interfacial properties, it is non-flammable, it is non-toxic, allows gas to pass through, compatible with optical detection, and it is commercially available [23]. PDMS is not hygroscopic, i.e. it does not swell with humidity. It has good thermal stability i.e.up to 186 °C

in air. Due to homogenous and isotropic nature of PDMS, they can be deformed mechanically to change the pattern and relief structures present on their surfaces [28].

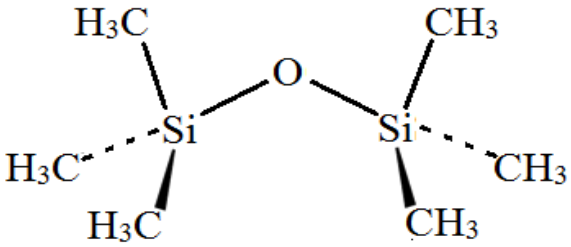

Figure 3.1: Structure of Polydimethylsiloxane (PDMS).

Plasma treatment of PDMS

The methyl groups present on the surface of PDMS makes it hydrophobic. Various techniques like chemical vapour deposition of polymer coatings, incorporation of an amphiphilic surfactant in the PDMS bulk, deposition of glass-like layers on the substrate surface (sol-gel coating), and layer-by-layer (LbL) deposition of charged polyanions and polycations have been used to modify surface properties of PDMS stamps. One of the most frequently used methods is plasma treatment/oxygen plasma. It is known that PDMS has a repeating unit of -O-Si(CH3)2- When PDMS is plasma treated, silanol groups are introduced that eliminates methyl group from PDMS. The addition of polar functional groups makes the exposed surface of PDMS highly hydrophilic [29]. As the oxidation of PDMS layer increases, the hydroxyl groups increase forming strong intermolecular interactions. However, this effect is only temporary, and PDMS again becomes hydrophobic several minutes after plasma treatment. The recovery of hydrophobicity of PDMS is due to the reorientation of the polar groups from the PDMS surface to the bulk, diffusion of pre-existing low-molecular-weight species from the bulk to the surface, and condensation of the hydroxyl groups. Apart from these reasons, as PDMS is a good elastomer its surface retains its hydrophobicity due to its elasticity. The recovery rate is also affected by storage condition such as temperature, humidity, aqueous fluid, and surfactants used to store the PDMS device [30].

Plasma treatment for a long time can cause cracking of PDMS stamps. These cracks are formed as a function of generator power, pressure and treatment time. Scanning electron microscopy has been used to characterize the cracks [31].

I. Molding

Patterned silicon wafers are used as a master, are used as templates for fabrication of elastomer stamps. The photoresist-coated wafer is referred to as the master or the master mould. The production of PDMS is shown in figure 3.2. Semiconductor processing methods utilize high aspect ratio photoresist to pattern a master. Then a thin layer of photoresist is spin coated on a master. The resist is patterned on the wafer by UV lithography via exposing mask on it. Later, the resist is washed with the developer to obtain desired patterns on the master. At the same time, it is important to treat the master with silane vapour: these silanes add CH_3 or CF_3 groups to cap the OH groups of master and prevent adhering of PDMS to the master [32].

PDMS base is mixed with the curing agent in the ratio of 10:1, degassed under vacuum to remove air bubbles, poured onto the wafer and cured at an elevated temperature to form a solid, cross-linked elastomer in few hours. Afterthat, the PDMS stamp is peeled off from the master without being damaged. Thus, the obtained PDMS stamp should have an exact replica pattern of their master, it should be able to form conformal contact with the substrate, and the features of the stamp should be mechanically stable during inking and printing on the substrate [33].

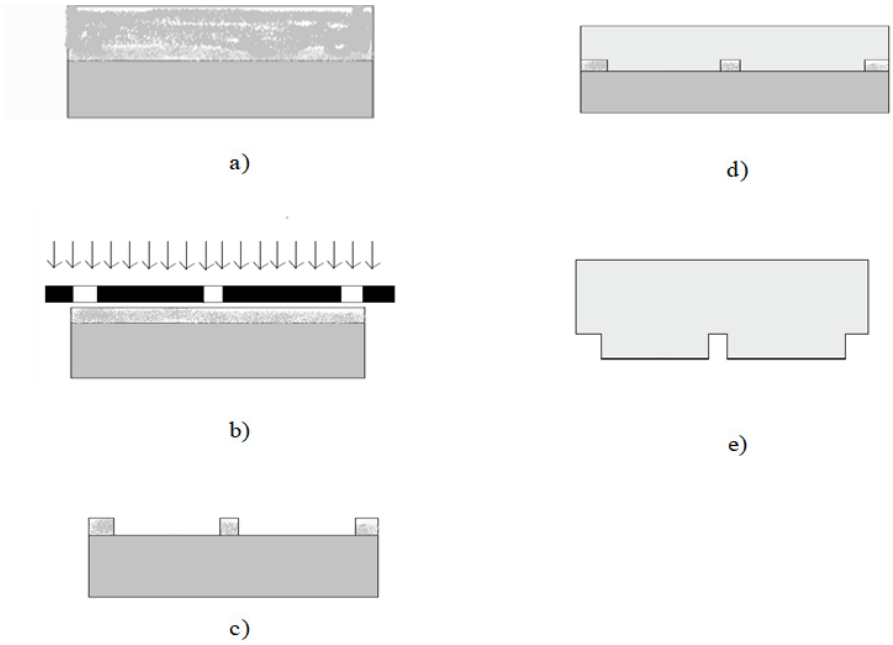

Figure 3.2: Production of PDMS stamp. (a) The photoresist is spun coated on a silicon wafer. (b) The silicon wafer is exposed to UV-light using a mask. (c) The exposed substrate is added to a developer, which dissolves photoresist, which is not cross-linked, and the master mould is produced with desired pattern. (d) The PDMS is casted on the master mould produced and is cured, and (e) The PDMS is peeled off from the master mould.

II. Printing

During micro-contact printing, the stamp is inked with the material or polymer to be printed by using inking techniques. Then, the stamp is placed in an inverted position onto a substrate. This leads to transfer of only the raised part of the stamp onto the substrate during the stamping process. A gentle pressure is applied on top of the substrate covering stamp, which helps to transfer the polymer thoroughly onto the substrate. The energy for binding polymers to the substrate should be stronger than the energy for molecules to stay on the stamp. Therefore, the surface chemistries of both the stamp and substrate are essential for the transfer efficiency [23]. The µCP process is demonstrated in figure 3.3. A typical stamp pad method decreased the swelling of the stamp and absorption of the molecules was also reduced on the surface after patterning. The self-passivating nature and low interfacial tension in the inked areas promote the formation of the self-assembled monolayers (SAM) instead of multiple monolayers. The SAM patterns avoid wet etching. Some conditions might require microcontact printing of hydrophobic ink onto the substrate as well. The inked areas are self-passivating and have a low interfacial tension that repels additional monolayers such that uniform self-assembled monolayers (SAM) are formed on the substrate. The SAM patterns act as a localised barrier to wet etching. Sometimes certain conditions require microcontact printing of hydrophobic ink onto the substrate [32].

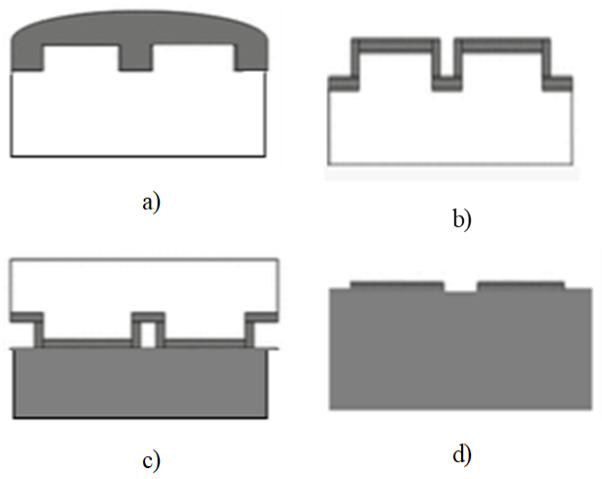

Figure 3.3: Schematic illustration of microcontact printing of polymer onto a substrate. (a) The PDMS stamps is inked with desired polymer. (b) The polymer is adsorbed by the PDMS stamp. (c) The stamp is placed pattern side down onto the substrate and gentle pressure is applied on top of the stamp. (d) The pattern of PDMS is transferred completely to the substrate.

3.2.2 Challenges of microcontact printing

μCP has certain limitations, most of them arise due to stamp deformations during the ink transfer. Roof collapse, buckling and lateral collapse are commonly encountered deformations, which are shown in figure 3.4:

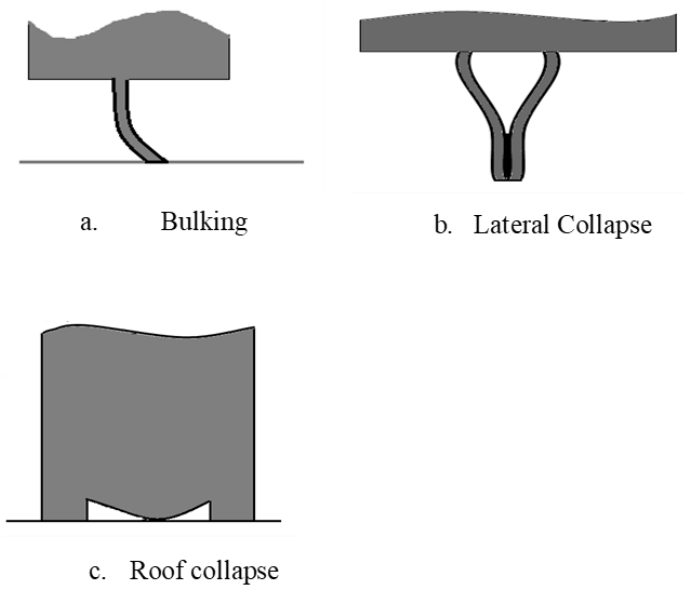

Figure 3.4: Different deformations of PDMS stamp. (a) Bulking (b) lateral collapse and (c) roof collapse.

The stamp can be deformed during its removal from the master or at the time of its contact with the substrate. Such deformations produce distorted patterns on the substrate that restricts resolution of patterning. Moreover, PDMS has low shear modulus ($G \leq 1$ MPa), so the features formed by microfabrication of silicon wafers do not form stable and functional structures on the stamp surface. As a result, different stamp deformations can occur. Three common stamp deformations are bulking, lateral collapse and roof collapse [34]. The rectangular cross-section of PDMS stamp is presented in figure 3.5. The features h, w and a was illustrated in figure 3.5 should be in the range of 0.2-20, 0.5-200, and 0.5-200 μm respectively. The order of aspect ratio to obtain deformation free PDMS stamps need to be 0.2-2 [28]. If the aspect ratio h/2a is too large, then the ridges can collapse resulting in bulking of stamps as shown in figure (3.4a). Another deformation, lateral collapse (figure 3.4b) of adjacent ridges can occur where liquid retained on the surface of stamp exerts capillary, forces which cause them to contract. Moreover, due to surface adhesive forces pillars may adhere to one another. The roof collapse occurs when the aspect ratio is too low. The roof of the stamp may come into contact with the substrate as shown in figure (3.4c).

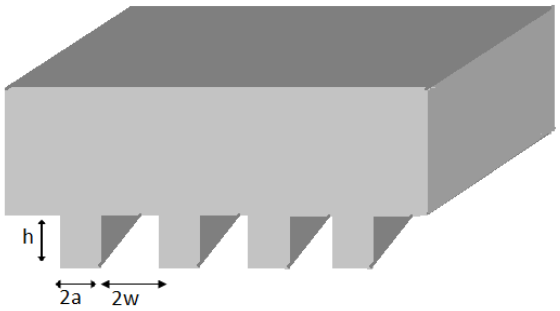

Figure 3.5: The rectangular cross-section of PDMS stamp. The stamp surface has flat pillars with width '2w', pillar height 'h' with pillar spacing '2a'in the range of micrometers or nanometers.

The conditions that must be satisfied to prevent above-mentioned deformations can be identified by using the following equations:

Roof collapse $$\frac{-4\sigma_{\infty} w}{\pi E^{*} h}\left(1+\frac{\alpha}{\omega}\right)\cos^{-1}\left[\sec\left(\frac{w\pi}{2(\omega+\alpha)}\right)\right]<1 \quad (1)$$

Buckling $$\frac{-12\sigma_{\infty} h^{2}}{\pi^{2} E^{*} \alpha^{2}}<\frac{1}{1+(\omega/\alpha)} \quad (2)$$

Lateral collapse $$\frac{h}{2a}\left[\frac{4\gamma_{s}}{3E^{*}\alpha}\right]^{1/4}<\sqrt{\omega/\alpha} \quad (3)$$

Here, σ_{∞} is the normal stress applied to the top of the stamp and $E^{*} \equiv E/(1-\nu^{2})$ applies to the plane strain modulus of the stamp material, where E implies Young's modulus and, v is the Poisson's ratio of the material. Besides, γ_s is the surface energy of the material, and 2a, 2w, and h are the features of the ridges representing width, spacing, and height respectively.

The equations 1, 2 and 3 were obtained assuming the surface relief has similar ridges with a rectangular cross-section. The axes of these ridges are parallel to the z-axis (i.e., the out-of-plane direction). The length of the ridges in the z-direction is assumed to be larger than w and a. The equation 3 is based on an other assumption that the ridges are of equal width 2a and are equally separated with spacing 2w along the x-axis [34].

3.3 Microbiology

3.3.1 *E. coli*

E. coli is an approximately 2μm long, peritrichously flagellated non-sporulating facultative anaerobic bacterium. It is a Gram-negative rod whose cell wall is made up of a thin peptidoglycan layer and an outer membrane. It is dominant in the gastrointestinal tract where it occupies mucus layer of the epithelial cells of the tract. *E. coli* grows with a generation time between 20 to 60 minutes, on a wide variety of nutrient sources at temperatures ranging from 8°C to a maximum of 48°C with a pleasant temperature of nearly 39°C. Because of these reasons, the bacterium is one of the best-characterized model organisms in biotechnology and microbiology. Most of the population genetic studies have used it as a prototype organism for decades as it is easy to culture and grow in the laboratory [35].

3.3.2 Cellular adhesion

Cellular adhesion is mediated by either specific interactions between receptors and ligands or non-specific interactions like hydrogen bonding, hydrophobic, van der Waals, electrostatic, and macromolecular forces. The capability of bacteria to adhere to various surfaces has been one of the principal processes by which they show pathogenic effects like harmful triggering of cellular signalling cascades, invasion of host cells, or biofilm formation. Urinary tract infections (UTI), caused by Uropathogenic *E.coli* (UPEC), is one of the most prevalent infectious diseases caused by bacterial adhesion. Adhesive organelles called fimbriae are responsible for the initial contact between the eukaryotic cell and the bacterium. Fimbriae consist of various protein units with a terminal lectin domain. These organelles are present on the outer membrane of the bacterium and project from the surface of UPEC. The bacterial adhesion to host cell is crucial for the subsequent development of the disease [36].

Fimbriae mediated bacterial adherence to host cells plays a crucial role in colonisation of the urinary tract. Uropathogenic *E. coli* exhibits different fimbriae: P, type 1, S, and F1C fimbriae. Mainly, P fimbriae and type 1 fimbriae are much-studied fimbriae, which help Uropathogenic *E. coli* (UPEC) to bind to carbohydrate receptors in the urinary tract. The carbohydrate receptors are mannose (or mannose-like) receptors found on the surface of the mucosal membrane [37]. The specific interaction of fimbriae of E.coli with mannan-coated surfaces is illustrated in figure 3.6. More than 80% of all Uropathogenic *E. coli* express mannose-specific Type 1 fimbriae [38].

Each type 1 fimbriated bacterium has 200–500 peritrichously arranged fimbriae on its surface, and each type 1 fimbria is a 7-nm-wide and ~1-μm-long. This fimbria has up to 3000 copies of the major subunit protein, FimA that is polymerised into a right-handed helical structure. Also, it has other minor components such as adapter proteins, FimF and FimG, and pilus adhesin FimH in smaller amounts [38].

FimH adhesin protein is situated at the tip of the fimbriae and is also embedded along the fimbrial shaft [39]. It has two significant domains; the N-terminal domain is the receptor-binding domain, while the C-terminal domain has the recognition sequences, which integrates into the outer membrane and forms barrel structure pore through which the N-terminal domain is extruded to the bacterial surface [39]. Also, the FimH protein is the receptor-recognising component of type 1 fimbriae, which binds to α-D-mannose-containing structures. The FimF and FimG help FimH adhesin to be integrated into the fimbriae. A high degree of flexibility is shown by FimH adhesin towards the identification of target organelle [40]. It recognises glycoprotein receptors with monomannose and trimannose residues. FimH components of commensal *E. coli* bind with high affinity to trimannose residues, while uropathogenic bacteria has FimH molecules that bind to monomannose residues with higher affinity. The combination of FimH with carbohydrate receptors is not only responsible for bacterial adhesion, but also bacterial internalisation is exhibited in the bladder cells leading to bacterial persistence and chronic urinary tract infections [41].

Bacterial adhesion forces can be either a long-range regime or short-range regime. The long-range regime is nonspecific interactions such as hydrophobic and charged interactions. These interactions are often responsible for the initial contact at separation distances more significant than 50 nm. At the same time, a short-range regime includes specific receptor-ligand interactions, which takes place at distances up to 15 nm [42].

3.4 Chemicals that promote bacteriological adhesion

3.4.1 Mannan

Mannan is one of the most important hemicellulose elements present in higher plants and seaweeds as structural and storage polysaccharide. As well as it is also a chief component of yeast cell wall composed of sugar mannose residues. It is known that a highly branched mannan polysaccharide has α (1-2) and α (1-3) linked side chains attached to α (1-6) linked backbone. Further, methods like methylation and degradative technique of acetolysis have been utilised to

study mannan structure. The mannan polysaccharides can be pure mannan (mannose only containing) and; glucomannans, galactomannans and galacto-glucomannans [43].

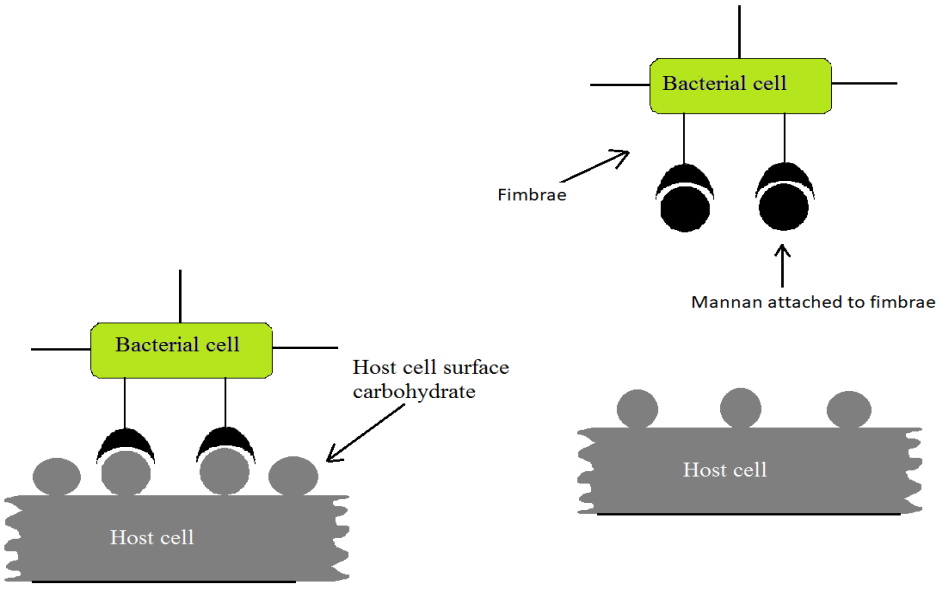

Figure 3.6: Schematic illustration of the interaction of bacterial fimbriae with mannan receptors present on host cell surface.

In order to functionalise surfaces with carbohydrates, chemical modification of the carbohydrate is sometimes needed. Reductive animation helps to convert carbonyl compound into amines directly. The reducing agent that is most widely used is 2-Picoline- borane (Pic-BH_3). It is a commercially available crystalline solid (mp 44–45°C) that is thermally stable to above 150°C. It can be purified by recrystallization from hexane and be stored for long periods without noticeable decomposition. It has properties such as it produces non-toxic wastes, it smoothly works in various solvents including water, it is highly selective and cost-effective make it a better candidate for reductive amination.[44].

3.4.2 Poly-L-Lysine (PLL)

Polylysine is a positively charged polymer of the hydrophilic amino acids: L-lysine or D-lysine. The structure of PLL is shown in figure 3.7. The precursor amino acid lysine contains two amino groups among which one is at the α-carbon and another one is at the ε-carbon. Polymerization can occur at either position resulting in α-polylysine or ε-polylysine [45].

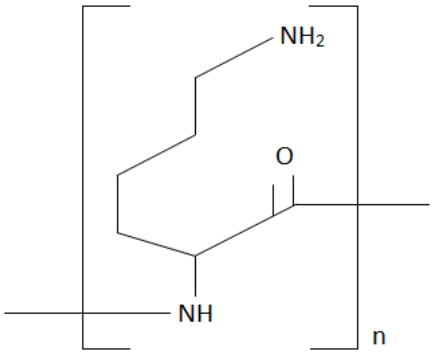

Figure 3.7: Structure of Poly-L-lysine.

PLL is biodegradable and biocompatible chemical. It is commonly used for surface coatings and delivery of the drug, gene and protein. Positively charged poly-L-lysine having cationic sites that attach firmly to anionic sites on cell surfaces as illustrated in figure 3.8. Additionally, when the chemical gets absorbed by the cell surfaces, these cells may remain alive but can be flattened. Along with cellular adhesion, PLL coated surfaces are also useful in adhering nucleic acids, proteins and enzymes. Further, it can be grafted with less adhesive molecules and improve their attachment to surfaces. PLL is quickly and easily adsorbed on different surfaces like glass, metals, metal oxides. The adsorption of PLL occurs by either simple diffusion from the bulk solution to the surface or conformational changes induced by repositioning of H-bonds and intramolecular charge distribution. Earlier research had shown that PLL is well adsorbed on polar and hydrophilic surfaces in basic pH exhibiting strong adsorption at pH 11, whereas they are poorly adsorbed in acidic pH. The factors influencing the rate of PLL adsorption are temperature, pH and ionic strength [46].

Studies carried out on bacterial attachment to PLL coated glass surfaces had demonstrated that the negative charges present both on the glass and on bacterial surfaces make the positively charged PLL polymer molecules very useful for attachment. The binding is so strong that the bacteria can persist to be immobilised against the lateral forces exerted by AFM tips during imaging. The primary purpose of such type of research is to study characteristic information of live bacteria in vivo, so bacterial properties should not be modified remarkably during bacterial attachment on surfaces. Apart from these studies, PLL is also noted for its anti-microbial activity. Moreover, it has been observed that thinner layer of PLL has less antimicrobial effects on *E. coli* than thicker coatings. Likewise, various investigations were also performed showing the effect of molecular weights on the adhesive properties of PLL. It was found that higher molecular weights of the polymer have larger adhesive forces. The PLL with a molecular

weight of 350kDa provided better attachment and was in solutions of concentrations 0.05-0.1% [47].

PLL solution is inexpensive and straightforward to immobilise on glass surfaces for cellular attachment. However, surface immobilisation is found to be usable for only two weeks as PLL covered glass surfaces are in fact sensitive to the quality of glass cleaning process and the lifespan of PLL surfaces is reduced with time. Additionally, high salt conditions can destabilise PLL layer as positively charged PLL molecules bind to the negatively charged glass surfaces through electrostatic interactions [48].

PLL attached to other molecule are commercially available like PLL-FITC, where FITC is an abbreviation for fluorescein isothiocyanate, which is a fluorescein derivative. It is one of the most frequently used fluorescent derivatives for biological studies due to its good solubility in water, and high absorptivity. FITC with an excitation maximum of 490 nm and an emission maximum of 525 nm can be detected by fluorescence microscopy [49].

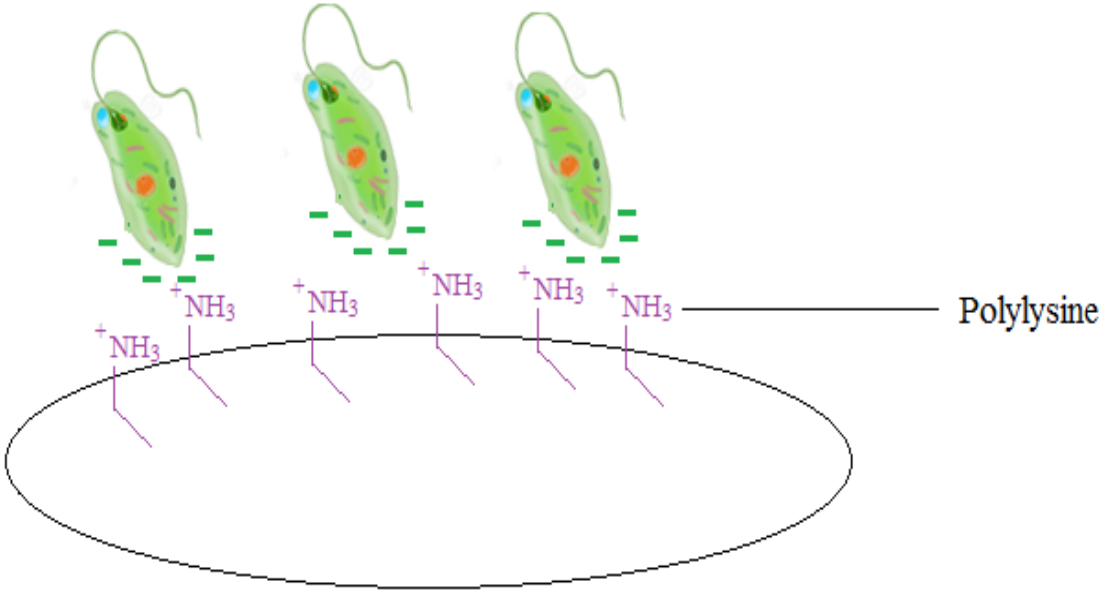

Figure 3.8: Schematic illustration of bacterial attachment to Poly-L-lysine.

3.4.3 Polydopamine (PD)

pH induced oxidative polymerization of dopamine produces polydopamine (PD) under alkaline conditions ((pH≥ 7.5). It is analogous to mussel adhesive protein, which can bind with high bonding strength to most surfaces due to the presence of catechol and amine-rich amino acids. It can bind to both cationic and anionic molecules as it acts as a zwitterionic polyelectrolyte. It

binds to amine-containing proteins in the outer membrane of Gram-negative and cell wall of Gram-positive bacteria. Amine groups are found both at a terminal end of proteins (N-terminus) and as side chains in multiple amino acids. Along with amine groups, it can also attach to thiols and metals. PD is of high interest for surface functionalization and coating for its chemical versatility, as it can interact with various surfaces through charge transfer and hydrogen bonds. It can also spontaneously adhere to many surfaces regardless of the chemical nature like mussel threads [50]. Among other molecules that PD can bind to include PVA and PEG, which allows it to be used for patterning on such surfaces as well. PD thus can be used as a coating material for adhesion and immobilisation of eukaryotic and bacterial cells on surfaces like PVA and PEG, which otherwise might resist adhesion. These chemical properties along with the inexpensive price, easy availability, adequate biocompatibility and low toxicity make it a prominent choice for the bacterial adhesion. Besides being capable of binding amine and thiol moieties PD can be used as the coating material to produce thin films by binding to molecules like PVA and PEG. This means the polymer can be used to pattern such surfaces and can act as the adhesive chemical to immobilise both eukaryotic and bacterial cells on surfaces which otherwise resist adhesion. Because of this property, it is selected as a notable contributor to the choice in a bacterial adhesive [51].

3.5 Chemicals that prevent bacterial adhesion

3.5.1 Polyethylene glycol (PEG)

$$HO\text{-}(CH_2CH_2O)\ N\text{-}CH_2CH_2OH$$

Figure 3.9: Structure of polyethylene glycol.

PEG is either a linear or a branched neutral polyether with different molecular weights. It is soluble in water and most organic solvents. Usually, PEG is viscous colourless liquid at Mw less than 1000 whereas it is waxy white solid at higher Mw. PEG commonly used in biotechnical and biomedical areas has Mw ranging from less than 100 to 20. 000. [52]

PEG is widely used as an inhibitor for biological adhesion like the attachment of proteins and cells to surfaces. One of the mechanism involves the formation of brush coating that generates the repulsive osmotic force and reduced mobility of the polymer chains leading to the steric barrier. This barrier refers to the loss of entropy in the brush, which makes the close contact of a bacterial surface to the substrate unfavourable thermodynamically. The brush coating arises

from the high-density packing of polymer leading to outward stretching of the polymer from the surface [53]. The other mechanism explains that the high mobility, flexibility and hygroscopic nature of PEG chains which resist the protein adsorption on the surfaces. Because of high mobility and swollen PEG chains, the protein molecules cannot penetrate PEG-coated surface layer and cannot reach the surface. Most importantly, as the PEG can be heavily hydrated, layers of water molecules can form on the surface with PEG. Therefore, it is entropically unfeasible for proteins and bacterial surface to be adsorbed to the polymer layer. The PEG can be co-polymerized/grafted to other polymers like PLL or polyacrylics, which can adhere to the contrary surfaces as a monolayer. This allows to generate varieties of other PEG-based surfaces that can be used as a passivation layer in generating the adhesive patterns for eukaryotic and bacterial cells [54]. Various papers have also described different strategies to acquire coatings of PEG molecules on the surfaces, which can be short-chain mixed self-assembled monolayers (SEMs), long linear PEG chains and multi-armed star-shaped polymers [54].

The inherent properties that make the PEG an appropriate candidate for the laboratory use include low interfacial free energy, lack of binding sites, highly dynamic motions and extended chain conformation. Moreover, it is non-toxic and harmless to active proteins or cells although it interacts with cell membranes. Easy chemical modification and attachment to outer molecules and surfaces, and when attached to other molecules it has little effect on their chemistry but controls their solubility and increases their size [55].

Furthermore, PEG is a polyether that autoxidises relatively rapidly, especially in the presence of oxygen and transition metal ions. Most biochemically relevant solutions contain transition metal ions. It was reported that PEG decomposed after exposed to air for one week at 45 °C and after one month at 20 °C. In vivo the hydroxyl groups of PEGs can be oxidised enzymatically to aldehydes and acids, allowing proteins and cells to attach. The susceptibility of PEGs to oxidation damage reduces their utility for applications that require long-term material stability [56].

3.5.2 Bovine serum albumin (BSA)

Apart from PEG, BSA can be used to prevent cellular adhesion on surfaces. The properties of BSA such as reduced adsorption of nonspecific proteins on the surfaces and negative net charge at physiological pH make it useful as cell repellent substance. Being negatively charged it can repel negatively charged bacteria by its electrostatic repulsion. Although it is known to hamper

bacterial adhesion, the molecule can interact with bacteria to an extent allowing bacterial motility and weak adhesion, while it does not bind irreversibly to surface structures of the bacteria.

Many mammalian cell studies use PEG and BSA as substrates to enhance the biocompatibility of a large number of microdevice surfaces because of their effective resistance to nonspecific adsorption of different types of biomolecules, colloids and even cells. While, these modifications can only temporarily reduce the bacterial adhesion, but ultimately allow bacteria to adhere to the modified surfaces [53, 57].

3.6 Imaging Techniques

3.6.1 Brightfield Microscopy

The bright field microscope is the simplest form of light microscope. It forms a dark image of the sample on a bright background. The microscope has different components: the light path is straightforward, which consists of a transillumination light source that is usually a halogen lamp in the microscopic stand, a condenser that focuses light onto the sample, an objective lens that gathers light from the sample and magnifies the image, and oculars to view the image produced by the objective. It is based on the principle of critical or Kohler illumination to illuminate the sample. Kohler illumination functions with the help of different optical components: the field lens collects the light from the light source and transmits the light beam to the condenser lens, the field diaphragm controls the diameter of the light beam emerging from the collector lens, the condenser lens collects the light beam and forms a cone of light that illuminates the specimen and the aperture diaphragm controls the diameter of the cone [57, 58].

The bright-field microscope enlarges an object and makes it visible to the observer. The ocular lens and the objective lens are used to obtain magnification. Most of these microscopes are provided with three objective lenses having magnifying powers of 10X (low power), 40X (high power), and 100X (oil immersion). The objective lens magnifies the images of the specimen and produces the “real” image. Then, the real image of specimen passes through the body tube into the oculars, which is magnified by low power and gives the final image. The magnifying power of the objective and the ocular lenses are multiplied to produce the total magnification of the specimen. A chosen magnification allows every small detail of the image to be resolved by the retina or photographic plate. The magnification larger than this shows no any extra details, and it is called as empty magnification.

Resolving power is the ability of the lens of the microscope to distinguish between two very close points. The resolving power is defined as the least distance between points in the object that can be distinguished in the image. Light microscopes have resolution on the order of 0.2 to 0.3 μm. Even a microscope utilizing UV light (λ= 230 nm) does not appreciably increase resolution [59].

N.A. (Numerical Aperture) is defined as the ability of the objective lens to gather light. It ranges from 0.25-1.4. The higher the N.A, better the light-gathering properties of the lens, and better the resolution. Moreover, larger N.A. values refer to smaller working distances. If N.A. value is above 1.0, it shows that immersion oil has been used in the lens [60].

The signal to noise ratio and the physiology of vision determine the contrast of the microscope. The signal is the image of interest whereas the noise is the background of light associated with out-of-focus images, light scattered by dirt on optical surfaces. The capacity of the eye or other measuring device determines the detectable contrast to observe fine distinction in colour and intensity on resolvable areas of the image. Usually, greater noise leads to higher signal intensity, which is necessary to produce a detectable image. Most histological and cytological techniques have been developed to compensate for the fact that cells in a visible light display a decreased contrast. Staining is a classic example of such techniques, both live and dead cell staining [59].

3.6.2 Phase contrast microscopy

Phase contrast microscope is relatively easy to operate and therefore often used as a routine method for studying live cells and any transparent objects. Furthermore, the growth and cell divisions and reactions of cells to different factors like drugs, radiations and other physical and chemical agents can be studied and observed by this microscope. It is particularly useful for imaging of specimens that give rise to very little refraction of the light that is characterised by a refractive index of the sample, which is not much different from their surrounding medium.

A phase contrast microscope brings changes in phase shifts in light, which passes through a transparent object to brightness changes in the image. These phase shifts can be seen only when they are visualized as brightness variations [61].

3.6.3 Fluorescence microscopy

A fluorescence microscope observes cells or tissues that are stained with a fluorescent molecule. In general, some molecules are capable of absorbing light of a specific wavelength and subsequently emit light with a longer wavelength This property exhibited by molecules is termed as fluorescence, which can be either primary or secondary. The primary point to a situation where the fluorescence is due to molecules naturally present in the object under investigation, whereas secondary fluorescence is due to molecules that have been coupled with the object under study to make it fluorescent. A fluorophore is a chemical compound that can re-emit light after being excited.

Three crucial events control the fluorescence process all of which occur on timescales that differ by several orders of magnitude. Firstly, a susceptible molecule is excited by a photon in femtoseconds. Secondly, vibrational relaxation of excited electrons occurs to the lowest energy level, which is much slower and measured in picoseconds. The final process where the photon

of a long wavelength is emitted and returned to the ground state in the relatively longer period of nanoseconds.

Although a fluorescent image is formed because of light emitting from the specimen itself, the illuminating beams that excite fluorescence are not directly involved in the formation of the image. During the fluorescence up to 90% of the light is lost in the microscope so, to get the better efficiency, illumination aperture must be large enough to allow the maximum amount of light to the specimen.

During the process of fluorescence, an indicator absorbs the photon, it gains energy and enters an excited state. It emits another photon a few nanoseconds later losing some energy. As a result, the emitted photon has lesser energy than the absorbed photon. Thus, the photon emitted from an indicator has a higher wavelength as compared to the excited (absorbed) photon. This energy difference is called the Stokes shift. In figure 7.2 photon with a short wavelength (blue line) has higher energy than light with a longer wavelength (red line). The fluorescence photo bleaches when the samples are viewed under a microscope and fades away. So, this is not permanent [62] [63].

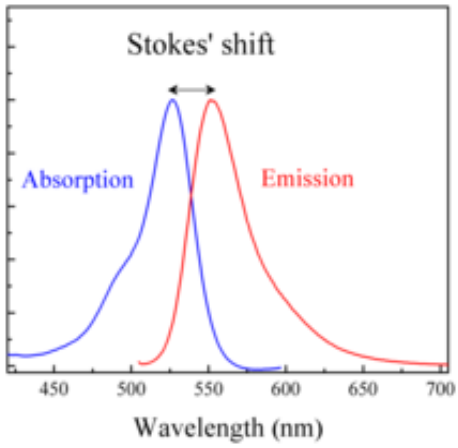

Figure 3.10: The absorption and emission spectra of a fluorophore. The Stokes shift of the spectra is indicated on the figure. The excitation light is of shorter wavelengths than the emission light. Adapted from [64].

3.6.4 Atomic force microscopy (AFM)

AFM images surfaces of objects at nanometric resolutions. It is still applicable for the visualisation of microcircuits, in material sciences and nanotechnology. It can be used to study complex biological systems like living cells, protein complexes, cellular membranes, viruses

and nucleic acids and meanwhile it quantifies and structurally map their biophysical properties at nanometer resolution. AFM contains a piezoelectric scanner, which brings the sample and tip into contact and separates them, and a cantilever with a small, sharply pointed tip, both are made up of silicon or silicon nitride, that moves over the sample surfaces, a laser beam that is reflected off the cantilever and measured by a photodiode. When the microscopic tip approaches the sample surface, the attractive forces cause the cantilever to deflect towards the surface. On the other side, repulsive forces are produced when the tip is sufficiently close to sampling surface deflecting the cantilever away from the surfaces. Photodiode measures the deflection of the reflected laser beam, and the interaction is recorded as force-distance curve [65, 66].

The attractive and repulsive forces between a microscope tip and sample surface are due to the interaction between a cloud of electrons in the atoms of the sample and the tip. These forces can be mechanical, Vander Waals forces, capillary forces, chemical bonding forces, electrostatic forces, magnetic forces, brush interactions, elastic interactions, or specific binding forces. Furthermore, these interactions are directly mapped to the topography of the biological sample. In addition, the tips can be physically, chemically or biologically functionalized [66].

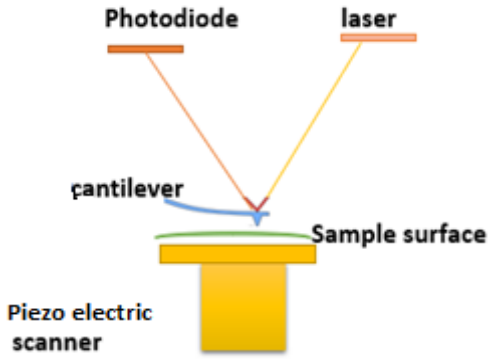

Figure 3.11: Working principle of AFM.

3.7 Quantification by AFM to produce Force-Distance Curve

AFM detects physicochemical and mechanical properties of the cell surface at a nanometric scale. AFM generates force-distance curves that record variations of interaction forces between the tip and sample surface when they approach each other, and the surface retrieves from the tip.

Figure 3.12 presents a force-distance curve obtained when allowing the AFM tip to approach and retract from a bacterial surface. As the microscopic tip moves across the cell surface from A to B, the adhesive force draws the tip down towards the bacterial cell surface at point B. As

the tip moves sufficiently near to the surface, the cantilever bends upwards. At point C, the sample retrieves from the tip and the cantilever bend downwards due to adhesion force until reaching the breakpoint at which the cantilever rebounds sharply upward to E. The adhesion force between the tip and surface is determined as follow:

$$F = k \times \Delta L$$

Where F is the force, k is the spring constant of the cantilever and ΔL is the deflection distance, which is the vertical distance between points D and A. Point A is the reference zero of deflection, when the tip is far away from the surface. A negative deflection corresponds to attractive force whereas the positive deflection corresponds to repulsive force [67].

AFM can be used to study specific and non-specific interactions that promote cellular adhesion. In case of the specific interaction between the microscopic tip and functionalised surface, the polymeric linker can join functionalising molecule to the microscopic tip. Then the separation of the tip from the sample first ruptures the nonspecific interactions between the tip and sample after which the linker is stretched until specific bond between the tip and sample ruptures. The rupture force of the specific bond can then be read out at a stretching distance related to the length of the linker.

On the other hand, hydrophobic forces play an important role for non-specific interactions. One of the study of yeast cells and hydrophobic substrates showed large adhesion force with extended rupture lengths which are characterized by non-specific binding and stretching of the hydrophobic tandem repeats of the adhesins [66].

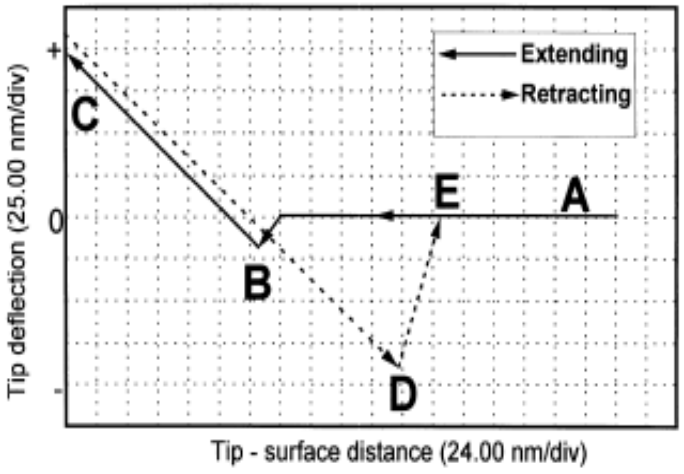

Figure 3.12: Force Distance curve obtained when allowing an AFM tip (continuous line) and then retract from (broken line) the surface of a bacterium.

4 Methods

4.1 Preparation of amine functionalized mannan polysaccharides

Materials

Saccharomyces cerevisiae Mannan (Sigma Aldrich), MQ water, methanol, picoline borane from Sigma Aldrich, 1M Acetic acid, 0.05 M NaCl, beaker, dialysis tube, clips, MQ water, electrical conductivity meter.

Methods

The mannan samples were dissolved in MQ-water to a final concentration of 3 mg/ml. Methanol was added to make a final concentration of 12% (v/v). 0.25M of the 2-methylpyridine borane complex (picoline borane, Sigma Aldrich) in methanol was then added to the final concentration of 24.24 mM. The pH was maintained to 5.8 using 1M acetic acid buffer. The samples were then incubated at room temperature for 48 hr. The excess reactants were removed by dialysis.

The dialysis tube was cut forming two open ends. One of the end was clipped and the amine functionalized mannan was added through the other ends of the tube and was clipped forming a bag 200 ml of 0.05 NaCl was added in 400 ml beaker to which the dialysis bag with mannan was soaked. It was left for 3 hours. 0.05 NaCl was replaced by another fresh 0.05 NaCl solution and left for another 3 hours. The solution was replaced by 200 ml MQ water every hour for 3 times. At the same time, the conductivity was monitored by electrical conductivity meter in between the experiment. The desirable conductivity is at least two μm. The solution was left overnight if it's conductivity was higher than 2 μm.

Finally, the samples were freeze-dried.

4.2 Preparation of cell culture and immobilisation of *E. coli* to mannan-coated glass surfaces

Materials

E. coli BL 21 cells and lysogenic Broth medium (LB) were kindly provided by Alex Wong a PhD working at the Department of Biotechnology and Food Science at NTNU. Live dead staining kit was provided by Swapnil Bhujbal, a Postdoc working at the Department of Biotechnology and Food Science at NTNU. The bacteria were grown overnight in LB medium.

Standard cover glass slides with size 24 mm by 50 mm or willCo-dishes or 96 well plates, 96% methanol, milli-Q water, N_2 gas, carboxylsilane (N-(trimethoxysilylpropyl) Ethylenediamine triacetic acid, ABCR GmbH and Co), 1 mM Acetic acid, amidized mannan, EDC (N-(3-Dimethylaminopropyl)-N' ethyl carbodiimide hydrochloride) from Sigma.

Methods

Initially, the willCo slides or 96 well plates were cleaned by placing them in a 1:1 v/v solution of puriss grade HCL (Sigma -Aldrich) and methanol (Sigma -Aldrich) for 20 minutes. The slides/plates were washed with MQ water for 5 minutes and dried by a steam of N_2 gas. They were then covered with 0.5 ml of 3% tricarboxylsilane dissolved in 1 mM Acetic acid and incubated for 30 minutes. The slides/plates were washed with MQ water and dried with steam of N_2 gas. Dried slides /plates were covered with 0.5 ml amidized mannan and 0.5 ml EDC and incubated for 30 minutes. The solution was drained off and dried with a steam of N_2 gas. The wilco slides were mounted to willCo dishes. 1µl of each component from the live dead Bac light bacterial viability kit were added to 900 µl of LB medium to which 100 µl of *E coli* culture were added. The culture was added to the mannan-coated surface and incubated for at least 30 minutes. It was rinsed with the LB medium 2 to 3 times to remove unattached bacteria. The LB medium was added to minimize stress on bacteria.

4.3 Photolithographic Process

Materials

2-inch wide and 279 µm thick Silicon wafers from Siltronix, wafer holder, tweezers, acetone, isopropanol, ethanol, a steam of N2 gas, hot plate, timer, washing beaker, cleaning wiper, Spin 150 Spin coater, MLA 150, mrDWL5 negative photoresist, mr DEV 600 developer, disposable plastic Pasteur pipette.

Method

The overall process of photolithography is illustrated in figure 4.1. Initially, the Si wafer was cleaned for good contact between the wafer and the mrDWL5 photoresist. The Si wafer was subjected to acetone bath. Tweezers were used to hold it and washed with isopropanol followed by ethanol. After cleaning, the wafer was blow dried with a steam of nitrogen. Subsequently it was exposed to oxygen plasma for 3 minutes to remove impurities and make the wafer hydrophilic. It was transferred to a hotplate at 180 °C for 20 minutes to dehydrate the surface. Once dried, the Si-wafer was placed and centred on the vacuum chuck in the Su8 spinner.

mrDWL5 photoresist was carefully applied onto the wafer by a disposable plastic Pasteur pipette held near the wafer, right above the wafer centre point. The spinner rotated at 3000 rpm for 33s. After spin coating the wafer was soft baked and placed on the hotplate set to 50°C. The set point was increased to 60°C. At about 55°C the set point was changed to 70°C. At about 65 °C the set point was changed to 80°C. At about 75°C the set point was changed to 90°C. The wafer was held at this temperature for 2 minutes. After which the set point was changed to 50°C again. The wafer was allowed to cool on the hot plate. When the temperature reached to 50°C the wafer was placed on a cleanroom wipe. It was left to relax for 10 minutes. After coating, the wafer was transferred to MLA 150 and exposed to 200 mJ/cm. After exposure, it was subjected for post-exposure bake. The wafer was placed on the hotplate that was set to 50°C. The set point was increased to 60°C. At about 55°C the set point was changed to 70°C. At about 65°C the set point was changed to 80°C. At about 75°C the set point was changed to 90°C. The wafer was held at this temperature for 2 minutes. After which the set point was changed to 50 °C again. The wafer could cool on the hot plate. When the temperature reached to 50°C, the wafer was placed on a cleanroom wipe. It was left for 1 hour. After exposure wafers were developed in mr DEV 600 for 1.5-2 min and the wafer is subjected to isopropanol bath for 1 min. The wafer was rinsed with isopropanol from squirt bottle while removing the sample. Then the wafer was dried with nitrogen gas. After which it was stored in the mask holder.

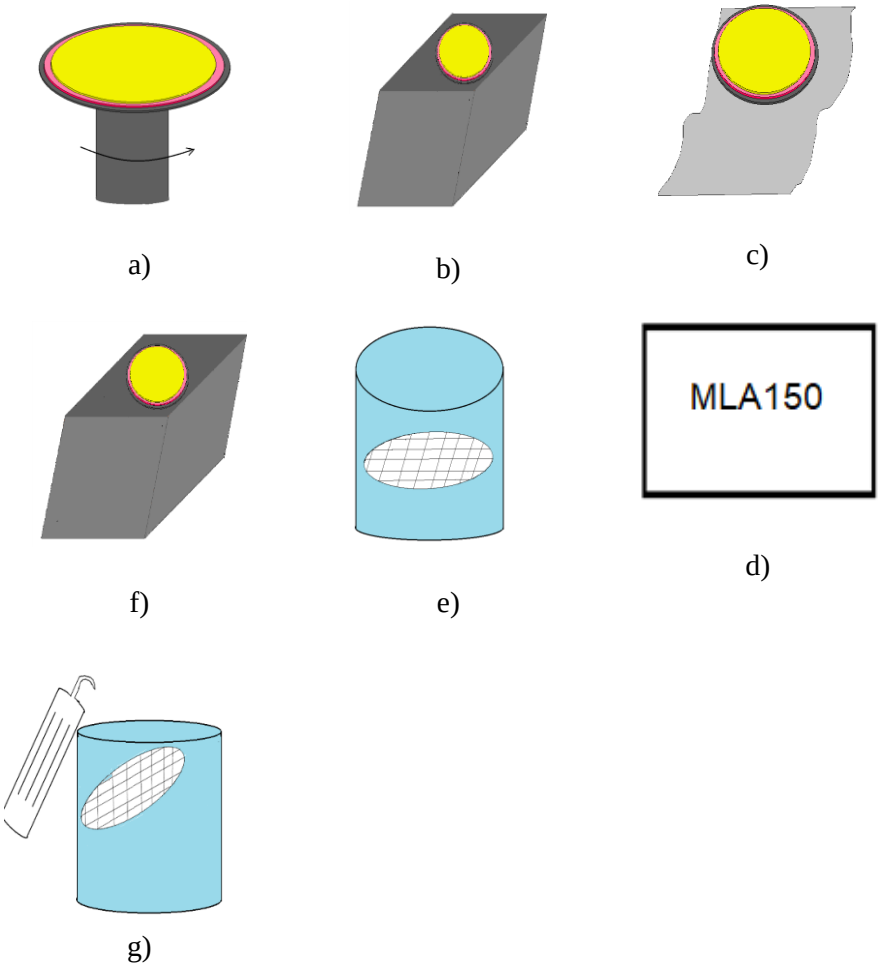

Figure 4.1: Illustration of photolithography process (a) the oxygen plasma cleaned silicon wafer is spin coated with the photoresist mrDWL 5 (b) the wafer is prebaked by placing it on the hotplate to dehydrate the surface (c) the wafer is allowed to cool on a cleaning wiper (d) the wafer is transferred to MLA 150 and exposed to 200 mj/cm after coating (e) the wafer is placed on the hot plate for post exposure bake (f) the wafer is developed in mr DEV 600 for 1.5-2 min after exposure, and (g) the wafer is subjected to isopropanol bath with squirt bottle for 1 min and then it is dried with N_2 gas and placed on the mask holder.

4.4 Stamp castings

Materials

Trichloroperfluorosilane from Sigma Aldrich, dropper, vial, silanization chamber, Sylgard 184 silicone elastomer kit from Dow Corning, petri dish, plastic cup, weighing machine, plastic spoon, vacuum desiccator, curing oven and master mold produced from photolithography.

Method

Initially, silanization of wafer was performed at NTNU Nanolab. 2 to 3 drops of Trichloroperfluorosilane was added to a small vial with a dropper. The vial was placed in the silanization chamber along with the master mold. The vacuum was turned on for 5 minutes so that the silane is evaporated in the chamber. After which, it was turned off for another 5 minutes to allow the master mold absorb the evaporated silane. The cycle was repeated for 3 to 4 cycles. Then, the mold was left in the chamber with vial for 1 hour with vacuum turned off.

After silanization, stamp casting is proceeded according to the following steps as shown in figure 4.2. First, the base and curing agent Sylgard 184 were filled in the plastic cup in the ratio of 1:10 with a dropper. The curing agent was poured first to maintain the optimal amount. The elements were thoroughly mixed for at least few minutes. Second, after mixing the elements, degassing was performed in the vacuum desiccator for 5 minutes. The plastic cup with mixture was put inside the desiccator. The vacuum was turned on using a vacuum pump or vacuum line. The cover of desiccator was checked. After 5 minutes, the vacuum was switched off. Once the pressure was stabilized, the cup was taken out the desiccator. The salinized mold was placed in the petri dish and PDMS was slowly added atop of the mold. The whole area of master mold was covered properly. The petri dish with master mold was put inside the preheated oven. The curing was performed at 65°C for 4 hours. The final step is to peel off the stamp from the mold. Scalpel and tweezers were used. First, all the borders were released using scalpel. The stamp is stored in the petri dish with the pattern facing upwards.

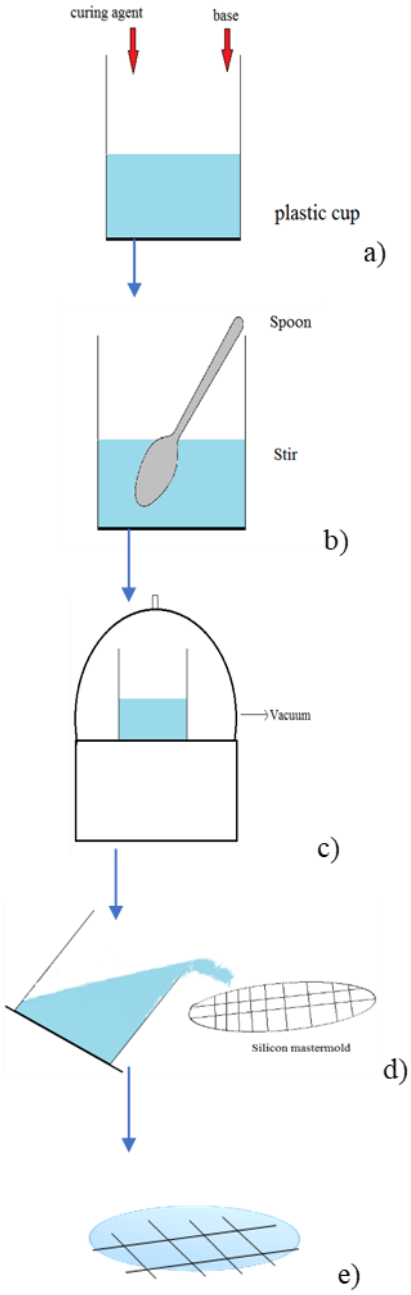

Figure 4.2: The process of stamp casting. (a) The PDMS containing base and curing agent are mixed in the ratio of 1:10 in a plastic cup. (b) PDMS is stirred with a spoon to remove bubbles. (c) The plastic cup with PDMS is placed inside the vacuum desiccator for 5 minutes. (d) PDMS is poured onto the master mold prepared from the soft lithography. Then, it is cured in an oven at 65°C for 4 hours. After which the stamp is peeled off from the master mold and cut by tweezers and scalpel. (e) The prepared PDMS stamp.

4.5 Functionalization of glass surfaces

4.5.1 Cleaning

Materials

Standard cover glass slides with size 75 mm by 25 mm or willCo-dishes, 96 % ethanol, milli-Q water.

Method

The glass slides or willCo-dish glass bottoms were rinsed with ethanol followed by milli-Q water and dried with Nitrogen gas. The cleaned willCo-dish glass bottoms were glued with a double-sided tape to form a complete willCo dish. They were covered with their lids to protect them from contamination.

4.5.2 Coating

Materials

Dopamine Hydrochloride from sigma, Poly-L-Lysine grafted polyethylene glycol (Pll-g-PEG) from SUSOS. BSA from Sigma Aldrich, Fluorescein isothiocyanate (FITC)-labelled poly-L-lysine (PLL), mw 15000-30000 from Sigma Aldrich. Poly-L-lysine (PLL), Mw 15000-30000 from Sigma Aldrich. Phosphate buffered saline (PBS) from Sigma Aldrich. Acetic acid. Milli-Q water. Tris buffer (pH 8.50) from sigma Aldrich.

Method

The cleaned coverslips, or willCo-dish bottoms were coated with Polydopamine Hydrochloride, BSA, and PLL-g-PEG, PLL.

Coating with Polydopamine hydrochloride (PD)

Dopamine Hydrochloride was dissolved in TRIS buffer to a concentration of 1mg/ml and vortexed. The glass coverslips, or willco dish bottoms were covered with the solution. The slides were incubated for 30 minutes. After incubation, slides were rinsed with MQ- water and blow dry with N_2 (g).

Coating with (PLL-g-PEG)

1 mg PLL-g-PEG was added to 1 ml MQ-water and centrifuged. The resulting solution was put on the slides and left to incubate for 1 hour as shown in figure 4.3. Then, excess liquid was removed by using the pipette. The slides were rinsed in PBS followed by milli-Q- water and blow dried with a steam of nitrogen gas.

Coating with BSA

BSA was dissolved in PBS to a concentration of 1mg/ml and kept on the slides for 20 minutes. The glass surface was washed off with milli-Q- water and dried with steam of nitrogen gas.

Coating with PLL

100 μL of the 0.01% PLL solution was placed on the slides for 10 minutes. The solution was then rinsed with MQ- water and dried with steam of nitrogen gas.The glass slides were coated with respective chemicals and kept in the petri dishes for later use.The coated glass slides were covered with BL21 *E. coli* cells and left for 20 minutes or more. The slides were then rinsed with LB medium for 2 to 3 times to remove unattached bacteria. LB was added to the slides to reduce the stress induced in the bacteria.

Coating of PDMS stamps

Materials

Dopamine Hydrochloride, Poly-L-Lysine grafted polyethylene glycol (PLL-g-PEG) from sigma. BSA from Sigma Aldrich, Fluorescein isothiocyanate (FITC)-labelled poly-L-lysine (PLL), mw 15000-30000 from Sigma Aldrich. Poly-L-lysine (PLL), mw 15000-30000 from Sigma Aldrich. Phosphate buffered saline (PBS) from Sigma Aldrich. Acetic acid. Milli-Q water. 10mM Tris buffer (pH 8.50) from sigma Aldrich, lysogeny broth growth medium (LB-medium), BL 21 *E. coli* cells overnight culture, 10 mM HEPES pH 7.3.

Method

A PDMS stamp was plasma cleaned /oxygen plasma with 50% oxygen gas and 100% generator power to reduce hydrophobicity between the substrate and chosen chemical; and to remove impurities from the surface of the substrate using an ionized gas plasma. A PDMS stamp was cut into small square (3mm by 3mm) by a scalpel. The stamp with the pattern facing up was placed on top of the glass side. A chosen chemical was deposited on the patterned stamp.

Coating with Polydopamine hydrochloride (PD)

1mg Dopamine Hydrochloride was dissolved in 1ml TRIS buffer and vortexed. The solution was left on top of the PDMS stamp for 30 minutes. After incubation, excess liquid was removed using micropipette and blow dried with nitrogen gas. The glass coverslips, or willCo dish bottoms were covered with the same solution for 30 minutes. After incubation, slides were rinsed with milli-Q- water and blow dried with N_2 (g).

Coating with PLL

100 µL of the 0.01% PLL solution was placed on the stamps for 10 minutes. The excess solution was then withdrawn with micropipette and the stamps were blow dried with a steam of nitrogen gas.

Coating with PLL-FITC

0.5 mg of PLL-FITC was mixed with 1 ml of MQ-water and vortexed. The solution was placed on the stamp for 15 minutes to dry it. Then, the excess solution was removed with a micropipette and blow-dried with a steam of nitrogen gas. The cleaned glass slide (no PLL-g-PEG) was placed on top of the patterned stamp. A pressure was applied on the stamp by placing a weight of 100 grams atop of the stamps to obtain good contact between the stamp and the slide. The weight was left on the stamp for 30 minutes or more after which the weight was removed from the stamp, and the underside of the slide was marked with a marker. Once marked, the slide is gently removed from the stamp.

4.6 Stamping

The stamping process is shown in figure 4.4. The stamps, coated with selected chemicals and dried, were placed pattern side down on the PLL-g-PEG coated slides to be patterned. A pressure was applied on the stamp by placing a weight of 100 grams atop of the stamps to obtain good contact between the stamp and PLL-g-PEG coated slides. The weight was left on the stamp for 30 minutes or more. After which the weight was removed from the stamp, and the underside of the slide was marked with a marker. Once marked, the slide is gently removed from the stamp.

4.7 Incubating bacteria

E. coli BL21 cells, diluted with LB medium, were added to the stamp patterned slides as shown in figure 4.4 (e). The cells were left on the patterned slide for 20 minutes. Subsequently, the

slides were rinsed with LB medium for 2 to 3 times to remove unattached bacteria. LB medium was added to the slides to decrease stress on bacteria.

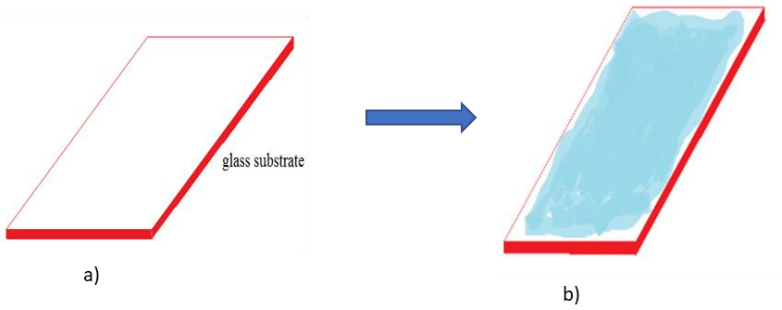

Figure 4.3: Illustration of passivation of the glass substrate - (a) the glass substrate (b) the anti-adhesive chemical is added to the glass substrate and incubated for specific time.

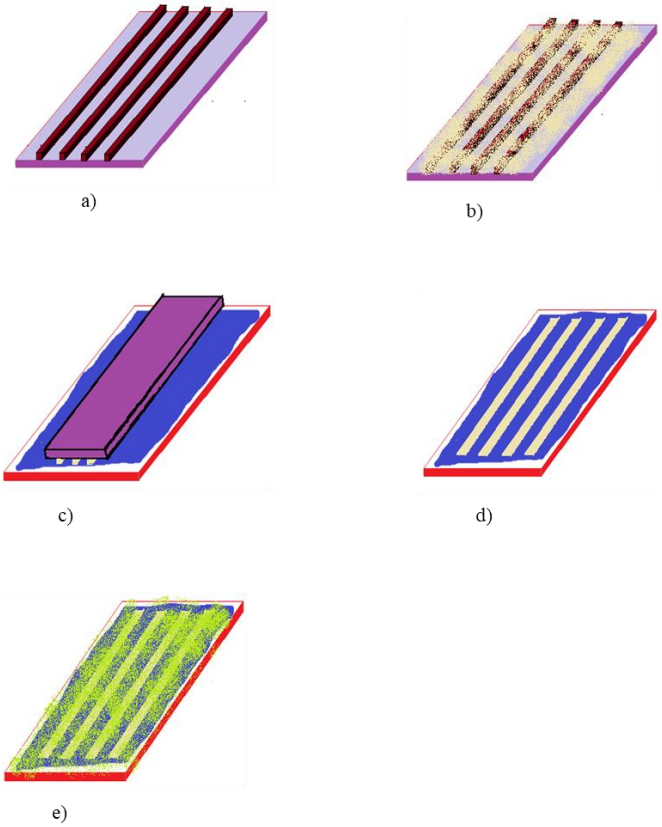

Figure 4.4: Illustration of microcontact printing process. (a) The PDMS stamp prepared from the master mold. (b) The PDMS stamp is incubated with chosen adhesive chemical, the chemicals are adsorbed onto the stamp forming a layer atop of it. (c) The stamp with an ink is pressed against the substrate for 15 minutes or more. (d) The ink is deposited to the glass substrate where they contact each other (e) The *E. coli* is added on the glass substrate with patterns and incubated for 30 minutes. The LB medium is used to wash away the unattached bacteria for 2 to 3 times leaving each bacterium deposited onto the substrate surface.

4.8 Quantification of adhesion strength between *E. coli* and mannan-coated surfaces using AFM

Materials

Dopamine Hydrochloride, TRIS buffer (pH8.5), MQ water, HEPES buffer (pH 7). All the materials for the experiment were purchased from Sigma Aldrich.

Methods

Initially, Dopamine hydrochloride (Sigma Aldrich) was dissolved in TRIS buffer (pH 8.5) to a final concentration of 1mg/ml. The AFM tip was then functionalized with polydopamine for 30 min to allow polymerization into polydopamine. *E. coli* cells were harvested by centrifugation (4000 rpm, 10 minutes) and washed twice in MQ water. The cells were re-suspended in MQ water. The cell suspension was inoculated on the functionalized tip for 20 min before washing in HEPES buffer (10 mM, pH 7). The tip was kept in HEPES buffer until measurements were performed to prevent drying of the cells. The presence of bacteria was confirmed by light microscopy inspection. All force-distance measurements were performed in HEPES buffer (10 mM, pH 7).

5 Results

In the present study, different adhesive and anti-adhesive chemicals were investigated. The adhesive chemicals were mannan, polydopamine and PLL whereas anti-adhesive molecules were BSA and PEG in addition to clean glass surfaces. The bacteria investigated were originated from overnight cultures of BL21 *E. coli* cells in LB medium. The glass surfaces coated with these chemicals were covered with bacterial suspensions. LB medium was used to cover the glass surfaces with bacteria and imaged using Zeiss Z.1 Axio observer light microscopy. They were imaged with 20 X magnification. The fluorescence used was SYTO 9 and Propidium iodide.

5.1 Immobilisation of *E. coli* on aminated mannan-coated glass surfaces

Figure 5.1 shows the images of BL21 *E. coli* cells immobilized in aminated mannan-coated surfaces. *E. coli* cells were left on top of on an aminated mannan-coated glass surfaces for 3 hours. Images were obtained after 30 minutes incubation of *E. coli* cells. The study showed that high density of bacteria was attached to the surfaces already after 30 minutes, but the density further increased with time (data not shown).

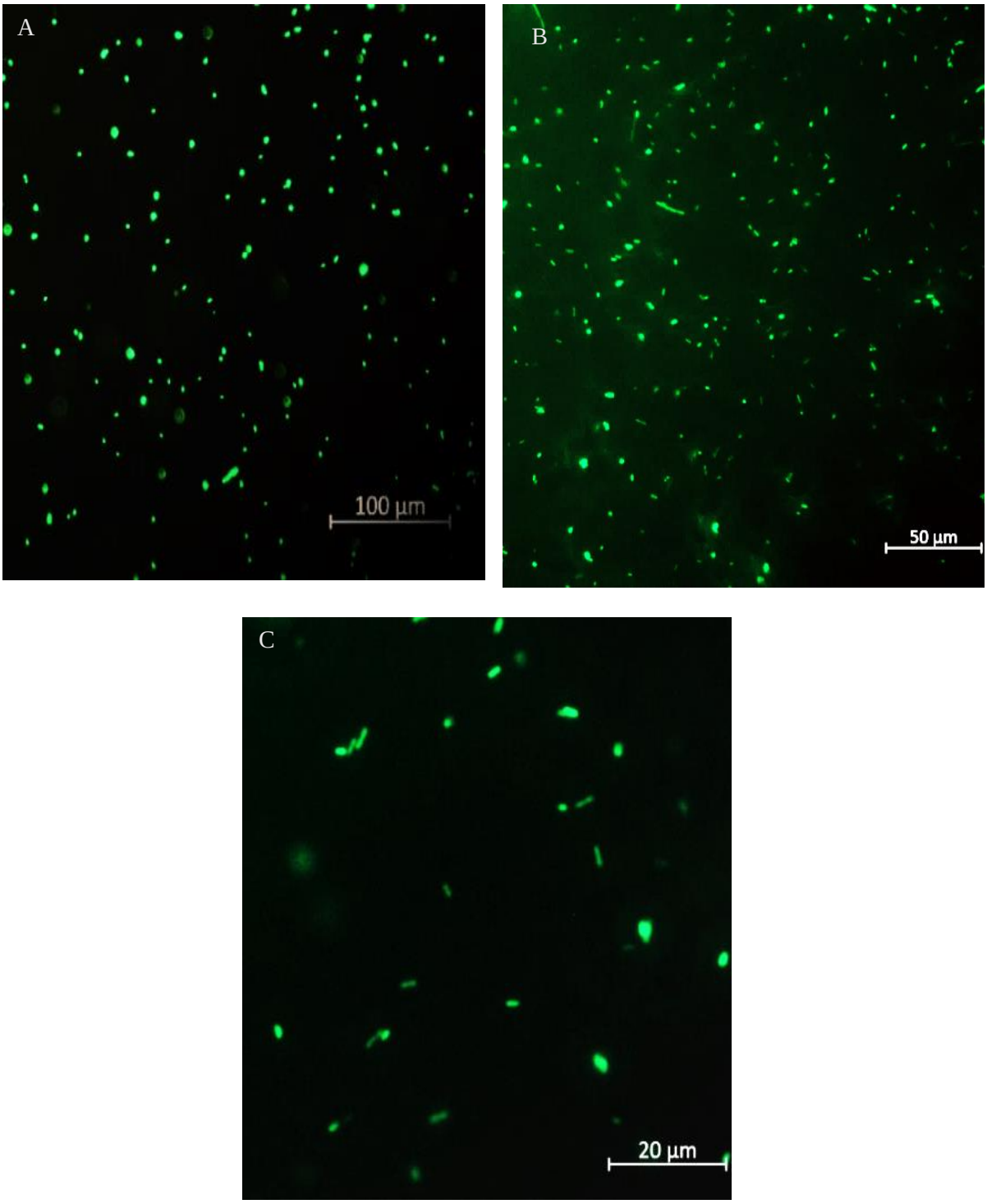

Figure 5.1: BL 21 *E. coli* cells immobilized on aminated mannan-coated glass surfaces. The images are obtained with fluorescence microscopy with a 20X (A), 40X(B) and 100X(C) magnification.

5.2 Immobilization of *E. coli* on different adhesive chemicals

A solution containing BL 21 *E. coli* cells were added on glass surfaces coated with different adhesive chemicals. The solution was left for 30 minutes. The resulting density of bacteria on

the functionalised surfaces was determined using fluorescence microscopy. The images obtained revealed that the highest density of bacteria was observed for aminated mannan-coated surfaces figure (5.2 A). A lower density was observed on polydopamine surfaces figure (5.2 B), and very few bacteria were observed on the PLL coated surfaces figure (5.2 C).

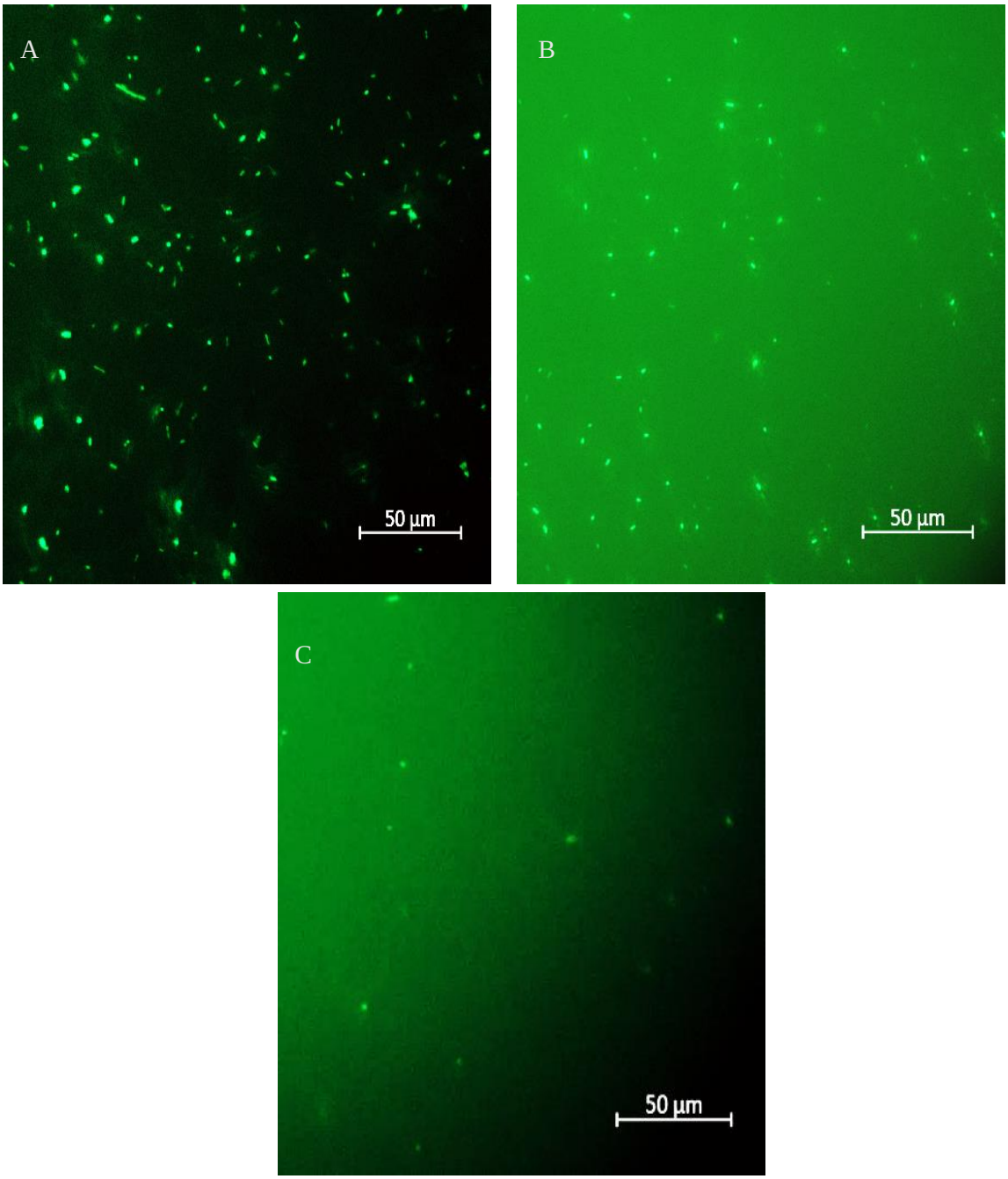

Figure 5.2: BL 21 *E. coli* cells immobilized to glass surfaces coated with aminated mannan (A), polydopamine (B), and PLL (C). The images are obtained with fluorescence microscopy with a 40 × magnification.

5.3 Passivation of surfaces

The glass surfaces coated with BSA (1mg/ml) in figure 5.3 (A) and PEG (1mg/ml) in figure 5.3 (B) revealed that fewer bacteria adhered to the BSA coated surface areas and PEG efficiently prevented bacterial adhesion. Some spots visible in figure 5.3 (A), and (B) below are due to the dirt present in the lens. Some bacteria in figure 9.1 are elongated in shape whereas others are oval and flattened in shape.

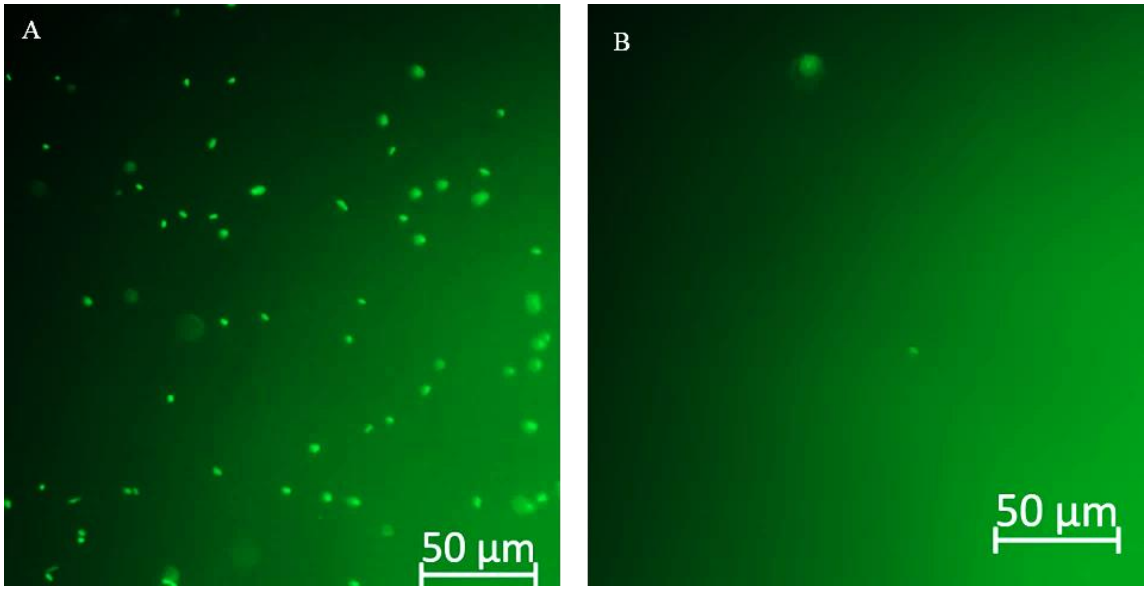

Figure 5.3: Immobilization of the BL21 *E. coli* cells. Overnight culture of BL21 *E. coli* cells immobilized on cleaned glass surfaces coated with BSA (A), and PEG (B). The glass surfaces were covered with LB medium after incubation of bacteria. Figure (A) and (B) show images obtained using fluorescence microscopy. The images were viewed in light microscopy with 40x magnification.

5.4 Characterization of stamps

PDMS stamps were prepared using master mold prepared by master student Kertu Liis Krigul. The master mold had varying circles of different diameter 4, 5, 6 and 7 µm with 10, 12, 14, and 16 µm separation distances between them. mrDWL 600 photoresist was used to create the pattern on the master mold. The PDMS stamps are prepared using the master mold. These stamps are imaged in a Zeiss Observer Z1 light microscopy at 20x magnification and the images obtained are presented in figure5.4. Image A, B, C and D in figure 5.4 display circles of varying diameters (4, 5, 6 and 7 µm) with 10, 12, 14, and 16 µm separation distances respectively, between them. The pattern was successfully transferred from the wafer to the stamp and was clearly visible under light microscopy. Some impurities, such as bubbles were sometimes

present in the channels present between circles (data not shown). On other stamps, the pattern was regular and defined over a large part of the stamp.

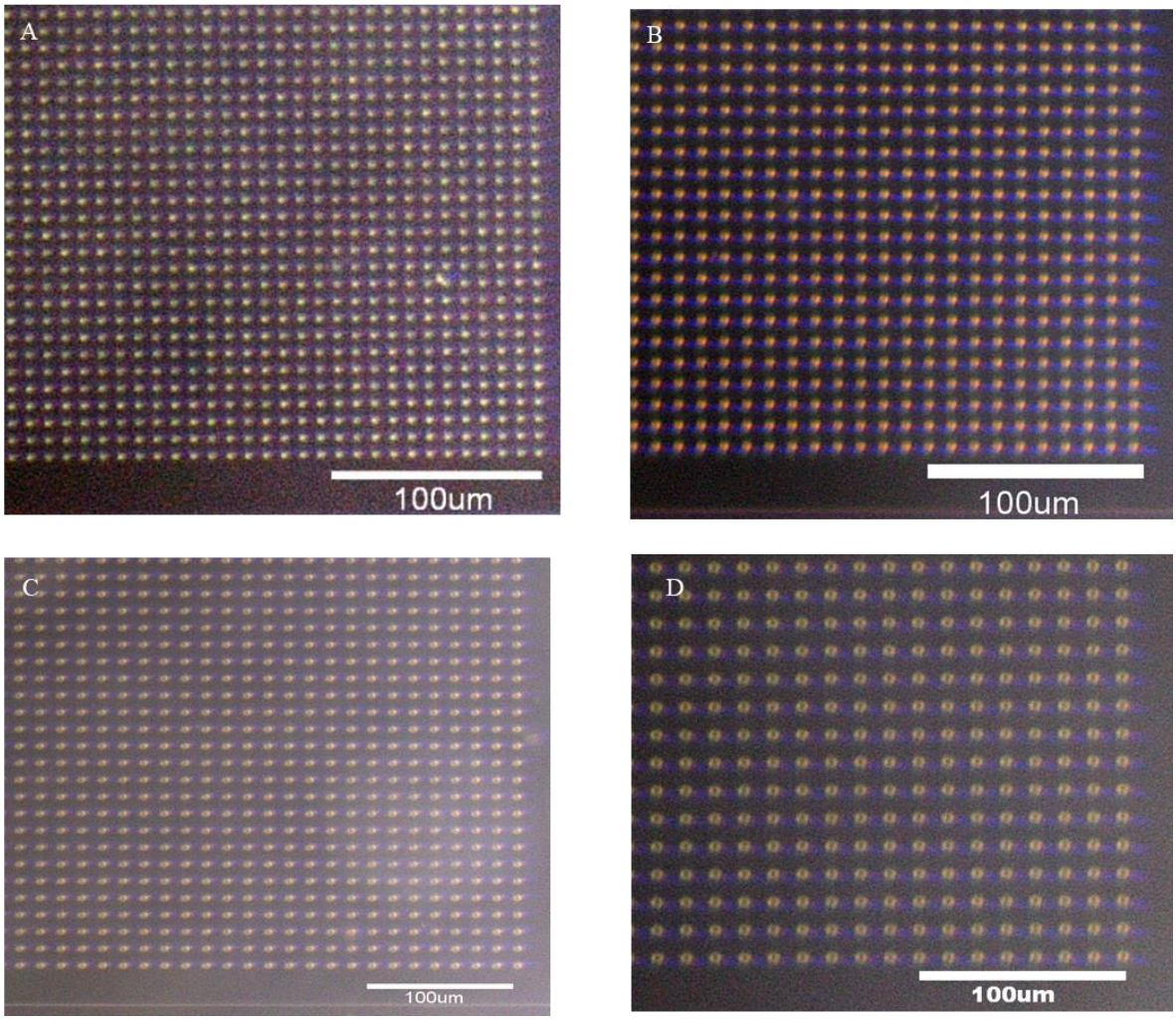

Figure 5.4: Image of PDMS stamps obtained using light microscopy with 20x magnification. The images reveal stamps with circles of different diameters and separation distances (A) pillar diameter equals 4 µm and separation distance between pillars equals 10 µm spacing, (B) 5 µm with 12 µm spacing, (C) 6 µm with 14 µm spacing and (D) 7 µm with 16 µm spacing.

5.5 Microcontact Printing

The successfulness of the µCP procedure was evaluated by observing the pattern obtained by stamping a fluorescent and non-fluorescent chemical on a glass surface. Later, BL21 *E. coli* grown in LB medium was added to the glass surfaces. The selected fluorescent chemicals were PLL-FITC (Sigma Aldrich), and non- fluorescent chemicals were PLL (Sigma Aldrich), mannan (Sigma Aldrich), polydopamine (Sigma Aldrich) and PLL-g PEG (Sigma Aldrich).

The stamp was fabricated by the master mold prepared by Kertu Liis Krigul. The stamp for μCP had different circles with a diameter of 4, 5, 6, and 7 μm with 10, 12, 14 and 16 μm separation distances respectively, between each circle. The images of microcontact printed glass surfaces were imaged by a Zeiss Observer Z1 light microscopy at 20x magnification.

5.5.1 Microcontact printing of PLL-FITC

μCP of PLL-FITC on clean glass surfaces showed regular micrometre patterns on the glass surfaces. Figure 5.5 (A) and (B) presents some representative results. The PLL-FITC spots were distinct and clear. The process was successful and readily reproduced with different diameters of the pillars on the PDMS stamp. FITC filter was inserted in the light path of the microscope to obtain the images of patterns in the fluorescence microscope.

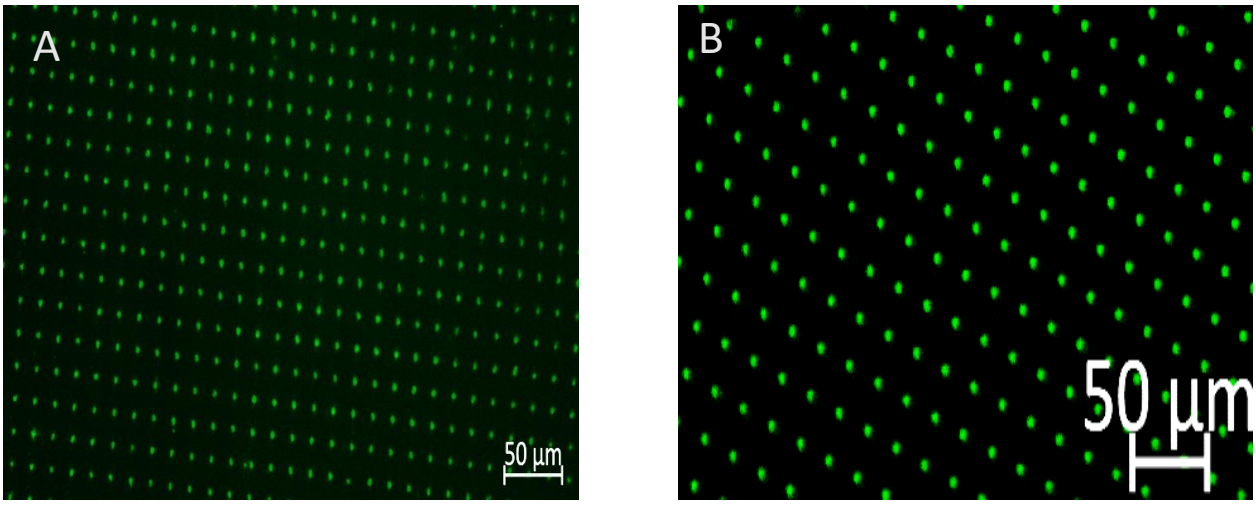

Figure 5.5: Microcontact printing on glass substrates with PLL FITC of circles with (A) 7 μm diameter and 16 μm separation distances (B) 5 μm diameter and 12 μm separation distances.

5.5.2 Microcontact printing of PLL-FITC with weights and no weights

The successfulness of μCP of PLL-FITC using mechanical pressure with tweezers, without applied weights and applying 100 g weights on top of the stamp for 20 mins was evaluated. The results are presented in figure 5.6 (A), (B) and (C) below. The image was obtained using the FITC filter on a Zeiss Observer Z.1 microscope. Figure (A) showed very light patterns. Although the patterns were copied, it is not clear and difficult to distinguish. Figure 2 does not show any patterns. The smearing of ink had occurred. A large droplet is seen in the middle of the glass surface. But some very faint dots can be seen on the very left side. No proper contact was established between the stamp and the substrate. Some of the patterns are smeared while

removing the weights from the glass surface. On the other hand, with 100 g applied pressure (figure 5.6 C) a clear pattern of 7µm circles with 15µm spacing is observed. The pressure was applied for 30minutes.

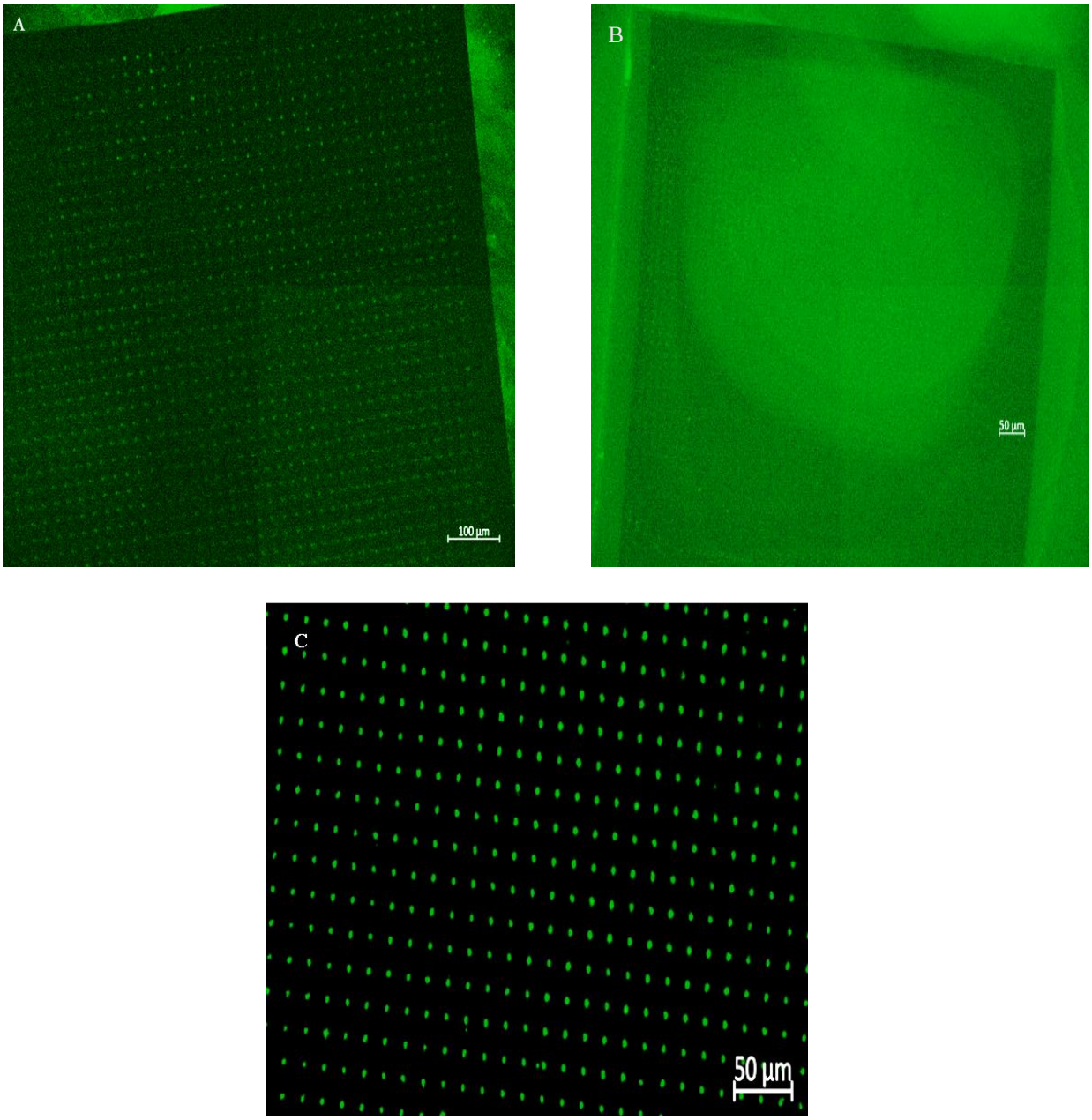

Figure 5.6: Microcontact printing of PLL-FITC on glass substrates (a) with weight applied by tweezers, (b) without an applied weight and (c) a 100 g weight was applied for 20 minutes during µCP to improve contact with the substrate surface. The image was obtained using the FITC filter on a Zeiss Axio observer Z.1 microscope.

5.5.3 Microcontact printing of PLL-FITC with plasma treated, and plasma not treated

Figure 5.7 shows microcontact printing of PLL-FITC with plasma not cleaned stamps (A) and the plasma cleaned stamp (B). The pattern is visible clearly in some of the areas, but these patterns are not copied properly all over the stamps. In B, the surface stamped with a plasma cleaned stamp for 1 min, the pattern is much clearer than for A and all the patterns were transferred completely on the glass surfaces.

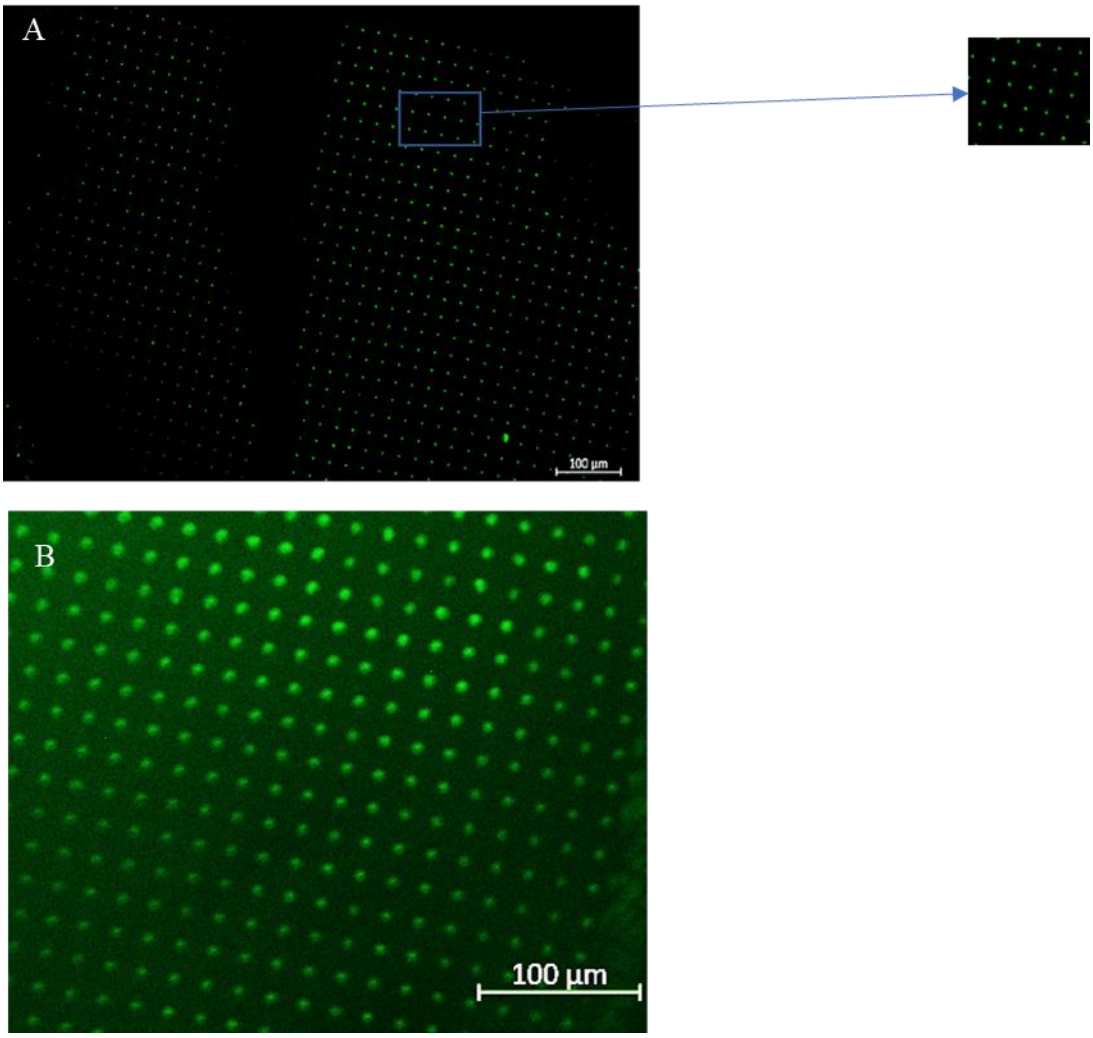

Figure 5.7: Comparison of the µCP stamps. Non-plasma treated (A), and plasma treated (B) PDMS stamp for µCP of PLL-FITC were compared. The PDMS stamps with circles of diameter 4 µm (A), and 7 µm (B) were used. The images were obtained using the FITC filter on a Zeiss Axio observer Z.1 microscope in 20x magnification for figure A and 40x for figure B.

5.5.4 Microcontact printing of PLL-g-PEG on PLL-FITC spots

µCP of PEGylated glass surfaces on PLL -FITC spots on the stamps manifested regular patterns with detailed images as shown in figure 5.8. The circles were exactly copied and printed on the

glass surfaces. The process was successful and reproduced easily. FITC filter was used to view the images of patterns in a fluorescence microscope.

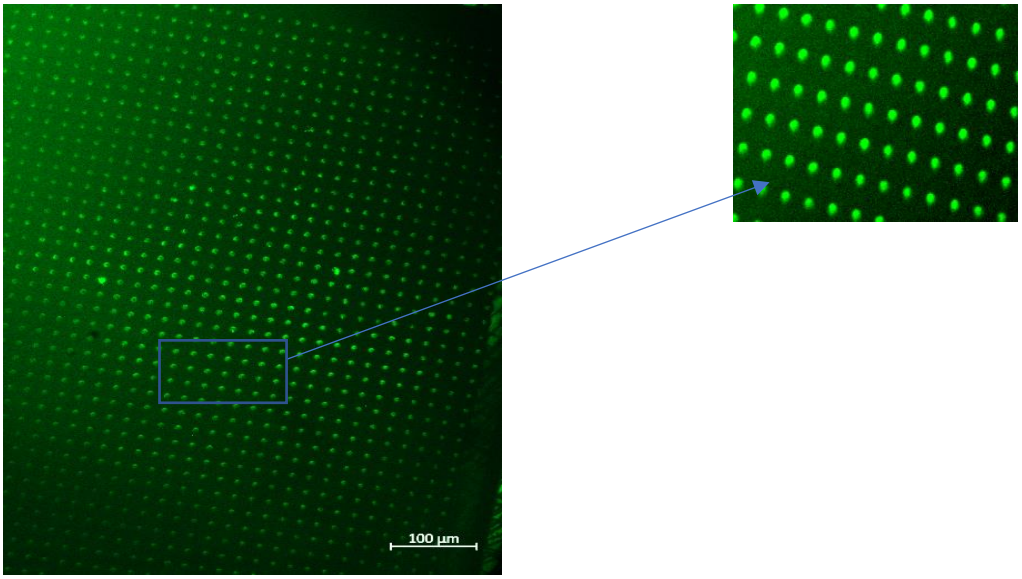

Figure 5.8: µCP of PEGylated glass surfaces on PLL-FITC spots over the stamp with diameter 7 µm with 16 µm separation distances.The images were obtained using the FITC filter on a Zeiss Axio observer Z.1 microscope with 20x objective was used.

5.5.5 Bacterial immobilisation on functionalised glass surfaces

Deposition of *E. coli* in PEGylated glass surfaces with polydopamine spots

An overnight culture of BL21 *E. coli* cells was added to the PEGylated glass surfaces with polydopamine spots and incubated for 30 mins. LB medium was used to wash away unattached bacteria after incubation for 3 to 4 times. *E. coli* cells were tagged with SYTO 9 and propidium iodide dyes.

In figure 5.9 *E. coli* cells were attached to the surfaces. A clear single bacterium can be seen but it didn't form the patterns. They were present all over the surfaces. A large aggregate of cells can be seen.

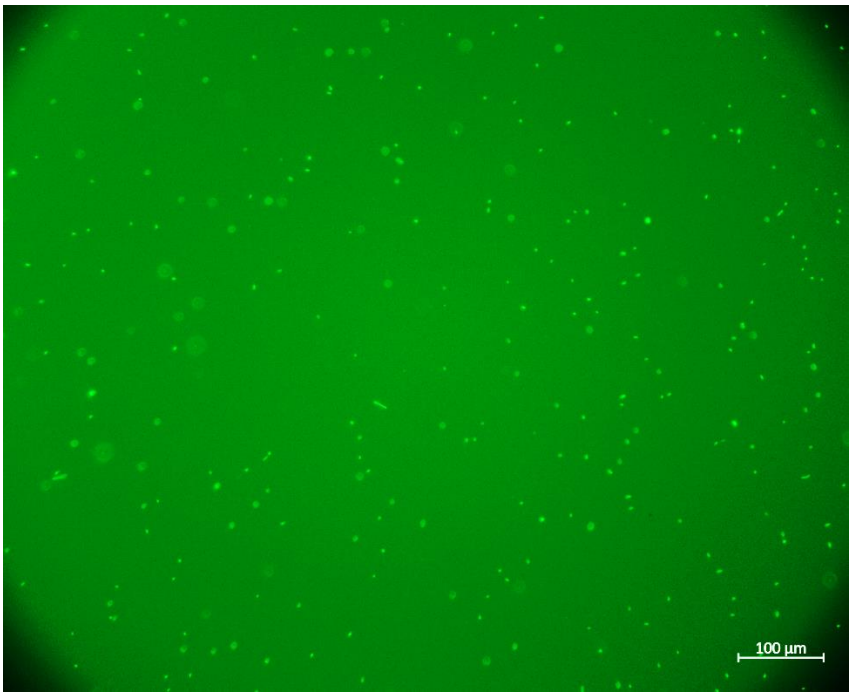

Figure 5.9: BL21 *E. coli* attached to the PEGylated glass surfaces with polydopamine spots. The surfaces were imaged using fluorescence microscopy with 20x magnification. The LB medium was used to wash bacteria. The image was observed in a Zeiss Axio observer Z.1 microscope with 20x objective.

Deposition of *E. coli* on PEGylated glass surfaces with mannan spots

E. coli cells did attach to PEGylated glass surfaces carrying mannan spots, but the position of the cells appeared to be random. They were present all over the surfaces. Most of the bacteria are present in a group. The rod shape of bacteria can be seen. 50mM HEPES buffer in 150 mM mannitol at pH 7.5 was used to remove detached *E. coli* cells. In figure 5.10 (B), *E.coli cells* were also attached to the surfaces. Some of the patterns can be seen in the middle part of the glass surface. Some of the cells are joined together and form a large elongated structure. Fragments of cells can be seen in some areas.

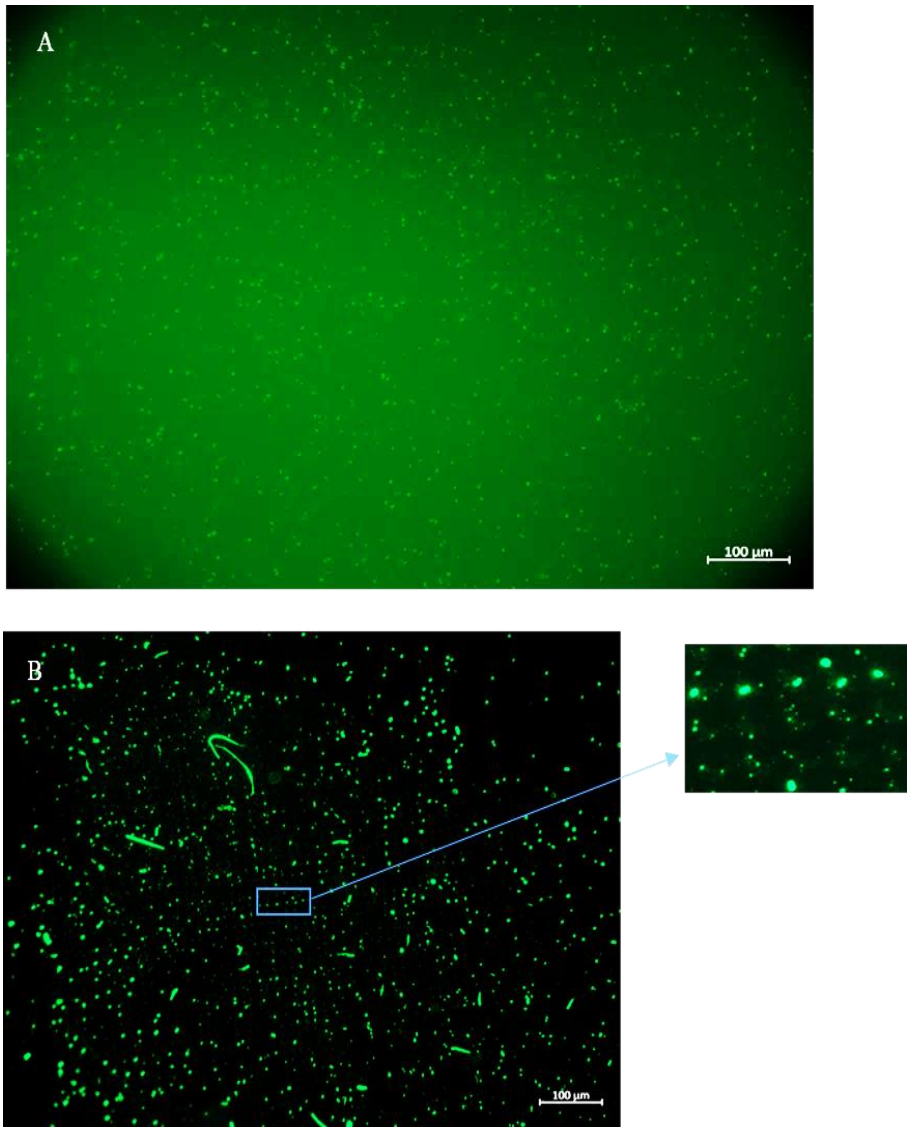

Figure 5.10: BL 21 *E. coli* attached to the cleaned glass surfaces with mannan spots (A) and to the PEGlated glass surfaces with mannan spots (B). The images was imaged using fluorescence microscopy with 20x magnification. In figure (A), BL 21 *E. coli* cells were incubated for 30 mins The LB medium was used to wash bacteria in figure (A) and HEPES buffer in figure (B). The circles were 4 µm in diameter with 10 µm gap between them. The image was observed in a Zeiss Axio observer Z.1 microscope with 20x objective. *E. coli* cells were tagged with SYTO 9 and propidium iodide dyes.

Deposition of *E. coli* on PEGylated glass surfaces with PLL spots

In Figure 5.11, the PDMS stamps with 7µm in diameter pillars were used to deposit PLL on PEGylated glass surfaces. *E. coli* cells did attach to the surfaces. They formed a regular pattern. Each spot is clear and distinct. The bacteria were fixed in each circle with their fimbriae moving. The rod shape structure of bacteria can be seen.in some of the spots single bacterium was

attached whereas other areas had more than a single bacterium. In some of the areas bacteria were washed away by LB medium leaving an empty space.

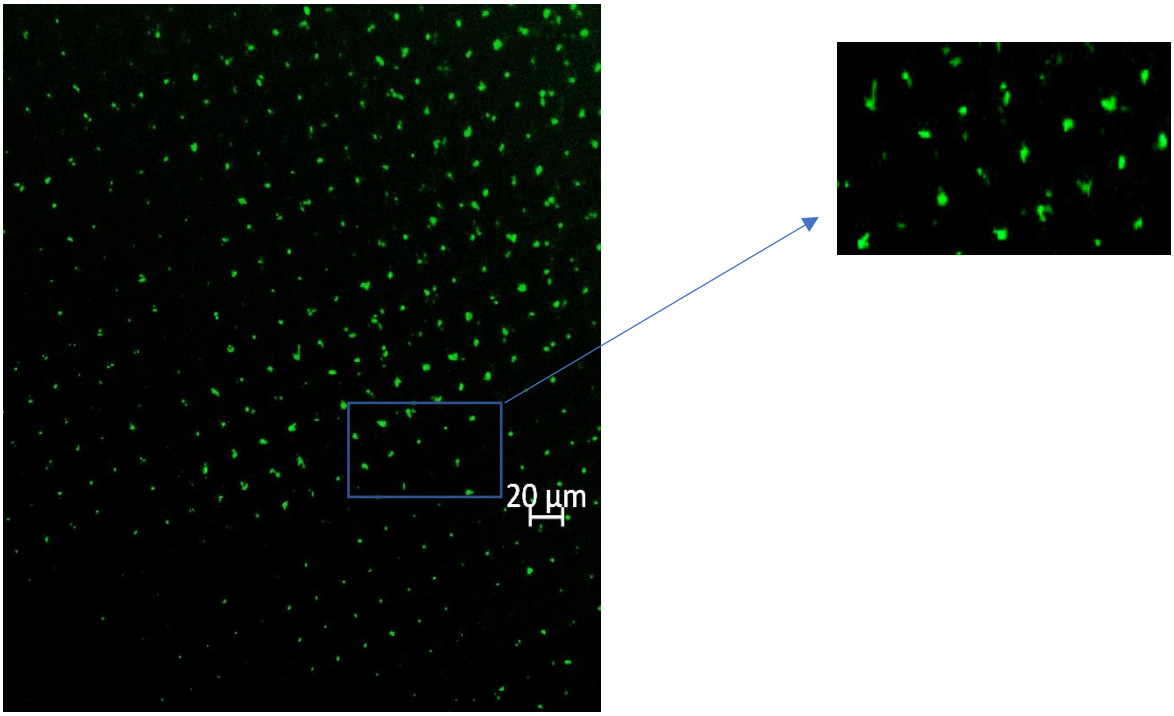

Figure 5.11: An overnight culture of BL21 *E. coli* attached to PEGylated glass surfaces with PLL spots. It was taken using fluorescence microscopy with 20x magnification. The bacteria were incubated for 20 minutes and washed 3 to 4 times with LB medium. The circles of PDMS stamps were 7 µm in diameter and 16 µm separation distances between them. The bacteria were stained with SYTO 9 and Propidium Iodide dyes.

5.6 AFM Analysis

5.6.1 AFM quantification of adhesion strength between *E. coli* and mannan-coated surfaces

AFM measurements were performed by PhD candidate Karen Dunker at the Department of Biotechnology and Food Sciences, NTNU. All force-distance measurements were performed on a Force robot 300 (JPK instruments) using a silicon nitride tip (Bruker, Germany) with length 180-220 µm, width 28-32 µm and spring constant (k) 0.02 N/m. The retraction speed was constant at 2 µm/s. The tip was coated with *E. coli* DH5α, kindly provided by post-doctoral fellow Swapnil Bhujbal, to create a bacterial probe. The same bacterial probe was used on both clean and mannan-coated glass surfaces.

Figure 5.12 (A) shows the interaction between structures on the surfaces of *E. coli* and the negatively charged glass surfaces. The contact point between AFM tip and glass surface is observed. This is when unspecific tip-surface interactions occur. The amount of interaction is higher between *E. coli* and the mannan-coated surface figure 5.12 (B) compared to *E. coli* and the glass surface figure 5.12 (A). The rupture events occur at a longer tip-surface separation distance. This means that larger surface structures are being stretched when *E. coli* interacts with the mannan-coated surfaces.

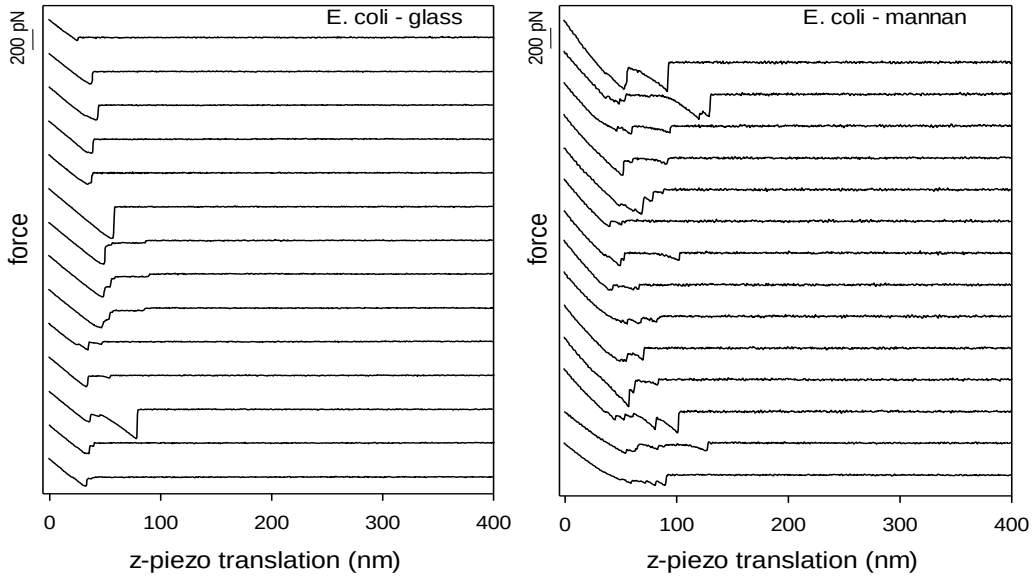

Figure 5.12: Representative force-distance curves of *E. coli* adhesion to clean glass surfaces (left) and mannan-coated surfaces (right). The results shown are from one experiment were 192 force-curves were recorded with the same bacterial probe on both surfaces. Force-curves were recorded over a 10 ×10 um sample area.

6 Discussion

The thesis work was initiated with an aim to develop a method for a bacterial microarray using a relatively simple, easy, cost-effective, reliable fabrication process. To accomplish the goal, the μCP was the selected method for preparation of patterned surfaces on the glass for selective bacterial adhesion onto predefined areas on the substrate. *E. coli* was used as the model organism. Although it is a well-studied organism with a short duplication time, the motility and cell size were limiting factors to develop a convenient and well-controlled method to make high-resolution arrays. For this purpose, μCP of different adhesive chemicals on a glass surface followed by an immobilization of *E. coli* on the functionalised glass surfaces was carried out. Most of the procedures utilized for μCP was based on work performed by Nina Bjørk Arnfinnsdottir at NTNU as part of her doctoral thesis.

6.1 Passivation of surfaces

The optimization of surface chemistry is important when it comes to controlling bacterial adherence in functionalised surfaces. In this thesis, the clean glass surfaces were investigated in the beginning as an anti-adhesive surface. An overnight grown culture of BL21 *E. coli* was placed on the glass surfaces leaving the bacteria in contact with the glass surface for 30 minutes, the solution was removed, and the surfaces were covered with LB medium to reduce the stress in the bacteria. The result showed that a clean glass surface did not prevent the attachment of bacteria. Instead, many bacteria adhered to the glass surfaces highlighting the need for passivating the surfaces. Two different anti-adhesive chemicals were therefore investigated: BSA and PLL-g-PEG.

6.1.1 Passivation with BSA

BSA did not provide effective anti-adhesion properties as can be seen in figure 5.3. BSA is known to decrease non-specific adsorption of proteins to surfaces. It has a net negative charge at physiological pH and was therefore expected to inhibit bacterial attachment by repelling negatively charged *E. coli* through electrostatic interactions. Protein lattice arrays of BSA was produced in micrometer scale by directly transferring BSA on glass surface from a PDMS stamp using μCP [53]. It was concluded that the notable decrease in cell adhesion on patterned areas is due to the steric repulsion forces exerted by BSA, which suppresses the interaction between bacteria and BSA. However, it is known that it attaches to bacteria and exhibits some adhesion.

The result obtained in the current study demonstrated that BSA does not entirely block the adhesion of *E. coli* to glass surfaces.

6.1.2 Passivation with PEG

PEG-coated surfaces are known to block bacterial adherence efficiently due to their protein resistance property. In this thesis, a PEG-grafted polymer with PLL backbone in a comb-like structure (PLL-g-PEG) was used. The PEG copolymer is deposited onto the glass surfaces by the electrostatic interaction between positively charged PLL and negatively charged glass surfaces. Thick and dense enough PEG copolymers attach covalently to the surface forming PEG brush. The brush forms a layer of polymer chains which is compressed when bacteria gets closer resulting in repulsive osmotic pressure and reduced mobility of the polymer chains. Park Ki Dong (1997) coated the surface of polyurethane with different molecular weights of polyethylene glycol and further studied two different bacteria *E. coli* and *S. epidermidis* in a variety of media. It was found that all PEG-modified surfaces lowered bacterial adhesion significantly and the range of adhesion differed depending on surfaces as well as media. Moreover, Eugene Liha (1998) has well explained about the flexibility and mobility as well as hydration of the PEG chains, which is responsible for their capacity to produce protein-resistant surfaces. Due to the high mobility of the surface-attached and swollen PEG chains, it is not possible for the protein molecules to penetrate into the surface layer and reach the surface to prevent the cell adhesion. From a different viewpoint, De Gennes *et al.*, with later expansion by Szleifer explained the effects of PEG on the inhibition of cell adhesion using the entropy model. Also, it can be noted that its repulsive property depends on the molecular weight (M_W) of the polymer and on the grafting density achieved, with higher concentration and higher M_W usually corresponding to higher repulsion [54].

The results provided in the current report add to and are in accordance with these results. This chemical was therefore chosen as a passivating agent for further process.

6.2 Microcontact printing with PLL-FITC

The μCP with PLL-FITC was started trying to observe the pattern by printing PDMS stamp with PLL-FITC onto clean glass surfaces. PLL-FITC is a fluorescent molecule. Earlier research had documented that PLL could immobilize bacteria onto glass surfaces, so this was assumed to be a better way to investigate whether the stamps made were appropriate for microcontact printing or not. Nina Bjørk Arnfinnsdottir had demonstrated that deposition of PLL-FITC by

microcontact printing is possible. The result obtained by N.B. Arnfinnsdottir were successfully reproduced in the current masterwork. PLL-FITC successfully transferred the patterns from the stamp to the cleaned glass surfaces as shown in figure 5.5 above. In addition, the result was reproduced repeatedly with different diameters of circular pillars. According to the previous research, μCP with small amounts of ink resulted in poor reproduction of the pattern and low fluorescence intensity [68]. As the amount of applied ink was increased, it became easier to apply the ink to the desired area of the stamp. Thus, relatively higher amount of ink (50 μl) was used and this procedure resulted in the successful transfer of patterns.

6.2.1 Microcontact printing of PLL-FITC with weights and no weights

In this master thesis, the effect of applying weight onto the PDMS stamp during the transfer of the chemical PLL-FITC onto the glass surface was compared. Once applying no weights, then gentle pressure applied using only tweezers, and finally, placing 100 g weights on top of the stamp with the pattern side facing down on the glass slides. When no weights were applied, smearing on the substrate was observed but when pressure with tweezers was applied, a light pattern of circles with PLL-FITC was observed in some areas whereas smearing occurred in other areas. In contrast, all the patterns were successfully transferred on to the glass slides with 100g weights. Based on this observation we concluded that under the last condition good contact between the stamp and the substrate was obtained. No patterns were lost, and no smearing was observed.

6.2.2 Microcontact printing of PLL-FITC on different time interval

Similarly, the residence time of the weights on to the glass slides also affected the pattern transfer to the cleaned glass surfaces. The patterns were less successfully transferred when weights were applied for 15 minutes while increasing the time to 20 minutes or larger improved the pattern transfer (images not shown). The increase in time allowed transferring all the patterns accurately. Therefore, we concluded that the printing of the pattern is dependent on the time duration for which the weight/pressure is applied.

6.2.3 Plasma treatment of PDMS stamps

The plasma cleaning improved the adhesion of PLL-FITC to the stamp and increased the transfer of chemical to the glass substrate. The PDMS stamp has a hydrophobic surface, which does not efficiently bind polar molecules and cause poor inking of the stamp. The ink solution

was accumulated in a single large drop when added in the stamps with no plasma cleaning. In addition, it did not cover all the area of the stamp, and it was time-consuming to adjust the chemical on top of the stamp. The plasma cleaning changed the surface of the stamp from hydrophobic to hydrophilic, and after this treatment, the solution was spread evenly across the stamp surface. Although it was time-consuming and tough to manage the ink over the stamp, the clear patterns were observed with plasma untreated stamps but with low intensity of fluorescence. Based on these observations it was concluded that, it is better to do plasma cleaning before using PDMS stamps for microcontact printing onto glass surfaces. The plasma cleaning at 50% O_2 and 100% generator power for 1 min was found to be more effective. Reduction in generator power to 50 % or less than 100% did not contribute much for hydrophilicity of PDMS stamps. According to the study carried out by M Brent (2008), PDMS overexposed to oxygen plasma: $t > 1$ min cause migration of low molecular weight hydrophobic species from bulk to the surface reducing hydrophilicity and forming cracks in the surface and making it rough. It was suggested that plasma treatment for 20-60seconds improve quality of adhesion due to increase in siloxyl groups on the PDMS surface whereas treatment for longer duration forms silicon dioxide on the surfaces decreasing the quality of adhesion. The recent study is in accordance with these results. Apart from this, plasma cleaned stamps are free of impurities on the surface producing smooth and clean PDMS stamps.

Plasma treatment of PDMS stamps showed effective results. However, this effect lasts only for 30 minutes. So, this step must be repeated every time before starting μCP. Although the surfaces of oxidized PDMS stamps can be made hydrophilic, repeated printing was not possible due to poor ink uptake by the hydrophobic bulk. Polyether ester was found to be much better at transferring patterns and form structures with clean walls and tops than oxidized PDMS stamps. In addition, it can perform repeated printing of patterns.

Silanization of the silicon wafer before casting PDMS onto it helped to peel off the PDMS stamps and prevent breaking of the wafer. Silanes deposited onto the silicon wafer reacts with silanols to form Si-O-Si bond with PDMS making it hydrophobic.

It was difficult to maintain a constant intensity of the steam of N_2 gas. A tiny piece of stamp was enough to carry out the process, so most of the time, a high intensity of N_2 gas blew away the stamp and had to repeat the process over.

After successful microcontact printing of PLL-FITC onto glass surfaces, PEGylated glass surfaces were microcontact printed with PLL-FITC. The patterns were successfully transferred

from the stamp to the PEGylated glass surfaces as shown in figure 5.8. The results were also reproducible.

6.3 Immobilization of *E. coli* on clean glass surfaces coated with different adhesive chemicals

Three chemicals promoting bacterial adhesion to substrates were tested and compared: Mannan, PLL, and PD. The clean glass surfaces were coated with the adhesive chemicals onto which overnight culture of *E. coli* BL 21 was added. After removing unbound cells, the glass surfaces with *E. coli* were covered with LB medium. Based on the results obtained it was concluded that *E. coli* BL 21 attached to all these chemicals. *E. coli* took a longer time to attach to the surfaces as compared to other bacteria like *Pseudomonas*. When left in contact with the surface for 5 minutes, the bacteria did not adhere to the glass surfaces coated with these chemicals. The contact time was therefore increased to 15 minutes, but still, all the bacteria were not fixed on the glass surfaces, some of them were mobile. Besides, it exhibited some adherence in 20 minutes, and all of them were stable on these surfaces in 30 minutes. The LB medium was added in between the experiment to decrease the stress on the bacteria. This liquid medium also prevented bacteria from drying out. The type 1 fimbriae of *E. coli* has Fim H lectin domains, which is specific to mannose molecules. On the other side, PLL being positively charged attach to negatively charged bacteria through electrostatic interaction. Although cells are alive, they may flatten which might be used for observational purposes.

These results obtained follows these hypotheses and demonstrate that immobilisation of *E. coli* is possible using these adhesive chemicals.

6.4 Micro contact printing-based deposition of Mannan, Polydopamine, and PLL on clean and PEGylated glass surfaces

The suitability of mannan, PD and PLL for the preparation of bacterial microarrays on both clean and PEGylated glass surfaces was tested with this experiment. Many bacteria were attached to microcontact printed clean glass surfaces, but they did not adhere exclusively to the adhesive spots. The bacteria seemed to be attached everywhere on the surfaces. There was no difference observed between the bacterial attachment to the cleaned glass surfaces and microcontact printed glass surfaces. It was therefore concluded that PEGylation of clean glass surfaces are necessary prior to deposition of these chemicals using μCP. Nina Bjørk Arnfinnsdottir was able to immobilize *P. putidas* on 3 μm spots of polydopamine. Her protocol was therefore followed when attempting to immobilise BL 21 *E. coli* on PEGylated glass

surfaces with PD spots. *E. coli* were labelled with the fluorescence SYTO 9 and PI introduced using live/dead assay kit. The bacteria were washed with LB medium for 3 to 4 times. When *E. coli* cells were added to the PEGylated glass surfaces with PD spots, *E. coli* attached everywhere. The pattern was not visible. In contrast, deposition of *E. coli* on PEGylated glass surfaces with PLL spots manifested adherence of bacteria predominantly to the spots. The PDMS stamps with 7 microns were used, which is larger than the bacterial size. Therefore, more than a single bacterium was attached to each spot. The bacteria seemed to be stable on the spots exhibiting mobility through their flagella. The result indicates that the PLL remained attached to the surface upon addition of suspended *E. coli* cells. The cells were evenly spread over the PEGylated glass surfaces with PLL spots and were immobilized in a distinct pattern. It was challenging to determine how many bacteria were attached to each spot. The results were attempted reproduced with 4 microns circles. The bacteria were adhered to all areas on glass surfaces with no visible patterns. The cells were expected to attach to the same spot where the PLL was applied, but they rather seemed to stay on the glass slide in groups or single, randomly around the surface. The bacteria were attached in the space between the circles as well. This could be due to the PLL-molecules detaching from the glass slide when the *E. coli* cells suspended in LB medium were added to the glass slide. Some of the PLL might have been washed away from the glass surface, while some of it stayed in place. The PLL used had a Mw of 150-300 kDa. Studies have found that PLL with higher molecular weights attaches better to glass surfaces than PLL of lower molecular weights. It is possible that PLL of higher molecular weights than used for this experiment would have had better attachment to the surface. Another possibility may be due to too thin polymer brushes of PEG, which might have permitted the interaction between the surface and *E. coli*. Also, the polymer brush which is not dense enough might cause chemicals like PLL to traverse through PEG chains and adhere to the surface underneath [69]. Therefore, it is thus possible denser or thicker PEG coatings might decrease unwanted attachment of bacteria.

Even though we are not able to reproduce the results, it indicates that adding PLL to a glass surface influence *E. coli* cell immobilization and these cells can be immobilised on PEGylated glass surfaces with PLL spots. The factors that are blocking the reproduction of the results with PLL spots are still unknown. The metabolic activity of bacteria is high at optical density 0.6, which means their motility is also high. This might have helped the *E. coli* cells to adhere to the glass surfaces. The LB medium due to its high ionic strength create a barrier for the attachment, so instead of LB medium, the *E. coli* cells that were deposited on the PEGylated glass surfaces with PLL spots were washed with 10mM HEPES buffer. The ionic strength of

the buffer is significantly lower than that of the medium. The resulting increased osmotic pressure might cause lysis of bacteria. Therefore, 70 mM mannitol was added in HEPES buffer with 1mM NaCl to balance the osmotic strength of the medium. However, the result obtained was not expected. Cells were attached forming various large aggregates randomly around the surface. Fragments of cells were seen in some areas, which can be due to the low ionic strength of HEPES. The flagella of cells were not moving as it was observed before with LB medium. It can therefore be assumed that most of the cells were lysed and fragments were formed with HEPES buffer. The experiment was continued with 50 mM HEPES, and 150 mM mannitol and further, it was diluted to 25 mM HEPES to 25 mM mannitol. Some spots were formed in some areas, but the same result was produced. This indicates that we were not able to optimize the ionic strength of HEPES buffer for the bacterial adherence. However, the results obtained with LB medium indicate that microarray imprinting of *E. coli* cells with PEGylated glass surfaces on PLL spots is possible.

BL 21 *E. coli* were deposited on PEGylated glass surfaces with mannan spots. The bacteria were attached everywhere with no regular patterns. One of the reasons may be that mannan did not attach to the stamps and consequently, no mannan was transferred to the surface. The bacteria were attached to some areas but most of the areas had lysed bacteria and the spots were fluorescently labelled. The lysis may be due to the lower ionic strength of HEPES. A similar result was observed for PD.

6.5 AFM analysis for the quantification of adhesion strength between *E. coli* and mannan-coated surfaces

The *E. coli* cells were attached to the AFM tip and moved towards and away from a clean glass surface and mannan-coated glass surfaces. The FD curve was obtained based on their interaction. Most of the FD curves obtained by the interaction between *E. coli* and clean glass surfaces are similar as shown in figure 5.12 A. This indicates that the cantilever holding the AFM tip is deflected towards the sample surface due to adhesive interactions formed between molecules on the AFM tip and structures on the surface of the bacterium. The obtained result is consistent with the hypothesis that rupture events occurred at a contact point between surfaces of *E. coli* and glass surfaces, and nonspecific interactions like hydrophobic forces showed large adhesion force with extended rupture lengths characterized by non-specific binding and stretching of the hydrophobic tandem repeats of the adhesins. These nonspecific interactions are responsible for extending the rupture lengths, which can be seen in figure 5.12 A.

On the other side, when the *E. coli* attached to the AFM and was moved towards the mannan-coated glass surfaces, most of the force-distance curves generated showed that the cantilever upon retraction from the surface is deflected towards the sample surface. The results in figure 5.12 B agrees with the hypothesis that *E. coli* interact with mannan-coated surfaces through Fim H mannan interactions. The Fim H is exposed at the end of type I pili explaining the observed rupture events at long surface tip separation distances.

The results revealed that both specific and unspecific interactions occurred between the *E. coli* functionalised AFM tip and mannan-coated surfaces. The separation of AFM tip from the sample first ruptures the nonspecific interactions between the tip and sample after which the pili is stretched until the specific bond between Fim H and mannan ruptures. The rupture force of the specific bond can then be read out at a stretching distance related to the length of the pili.

7 Conclusion

In this thesis work, microarrays of BL21 *E. coli* cells were obtained on PEGylated glass surfaces using PDMS stamps. During the study, *E. coli* cells deposited successfully on PEGylated glass surfaces with PLL spots of 7 μm diameter. The PDMS stamps with varying circles with diameters of 4 μm, 5 μm, 6 μm, and 7 μm with interpillar distances 10 μm, 12 μm, 14 μm, and 16 μm were used for μCP.

The microarray printing of PLL-FITC was successfully carried out on both clean and PEGylated glass surfaces, which confirmed that PLL could be used to pattern with micrometer resolution by μCP. The patterns were observed using fluorescence microscopy with a Zeiss Axiocam Z.1 microscope. In addition to PLL, *E. coli* cells were also able to attach to clean glass surfaces coated with mannan and polydopamine. Additionally, it was successfully manifested that plasma cleaning of the PDMS stamps improved the quality of μCP when compared to non-plasma cleaned stamps. A similar case was observed when applying weights on top of the stamp with the pattern side facing down on the glass slides. AFM study showed that Fim H present on the bacterial surface is responsible for adhesion between *E. coli* and mannan-coated surfaces.

Adding the step of silanization of silicon wafer helped the PDMS stamps to get removed from the microstructures of wafer easily without breaking the wafer. PDMS stamps are very hydrophobic, so plasma treatment of the stamps at 50% O_2 and 100% generator power worked effectively. As the plasma treatment lasts only for a short time, more hydrophilic stamps can be used instead of PDMS. Modification kits that induce permanent changes to the surface are commercially available and provide an alternative solution.

The main obstacle encountered during this project was related to the choice of the washing solution to remove unattached bacteria after incubation on microcontact printed PEGylated glass surfaces. Suitable washing medium or buffer for *E. coli* should be determined further for proper attachment of bacteria maintaining their viability. Once the appropriate washing buffer is identified, further steps can be carried out for proper micro-contact printing of *E. coli* on different chemicals. During the project, *E. coli* cells were able to form a regular pattern with PLL spots so, microarray fabrication can be initiated with PLL and then with other chemicals. Once *E. coli* cells are immobilised in a pattern, they can be used for single cell analysis for which the appropriate size of the adhesive islands as well as the separation distance between each island for *E. coli* can be determined. Afterwards, the growth rate of patterned *E. coli* cells can be determined. Furthermore, live/dead assay can be done to count live and dead bacteria.

This method is applicable in different areas like phenotypic variation screening, population evolution analysis, signal transduction-based pattern formation, cellular differentiation, metapopulation dynamics and others [18].

Lastly, microfluidics is an emerging technology to analyse small sample volume for which also immobilization of microorganisms is required. The bacterial microarray can be combined with a microfluidic device to monitor the liquid flow over the arrays. This can regulate the bacterial environment, and freely moving and unattached bacteria can be removed [70].

Once all essential parameters are managed, a future challenge is to develop methodologies extending to a multistrain bacterial array that would help study different dynamics in the complex ecosystem with individual/ population of different species. It enables to study in real time and with single cell resolution. This widens the possibility of different experiments and procedure which can create the practical and fundamental application in the field of nanobiotechnology, ecology, biosafety. Fundamentally, it should expand our knowledge pool on the ecological and evolutionary properties of living systems.

References

1. Lane, N., *The unseen world: reflections on Leeuwenhoek (1677)'Concerning little animals'.* Phil. Trans. R. Soc. B, 2015. **370**(1666): p. 20140344.
2. Koonin, E.V., *Does the central dogma still stand?* Biology direct, 2012. **7**(1): p. 27.
3. Altschuler, S.J. and L.F. Wu, *Cellular heterogeneity: do differences make a difference?* Cell, 2010. **141**(4): p. 559-563.
4. Paszek, P., et al., *Population robustness arising from cellular heterogeneity.* Proceedings of the National Academy of Sciences, 2010. **107**(25): p. 11644-11649.
5. Wang, D. and S. Bodovitz, *Single cell analysis: the new frontier in 'omics'.* Trends in biotechnology, 2010. **28**(6): p. 281-290.
6. Wang, Y. and N.E. Navin, *Advances and applications of single-cell sequencing technologies.* Molecular cell, 2015. **58**(4): p. 598-609.
7. Rubin, H., *The significance of biological heterogeneity.* Cancer and Metastasis Reviews, 1990. **9**(1): p. 1-20.
8. Grote, J., D. Krysciak, and W.R. Streit, *Phenotypic heterogeneity, a phenomenon that may explain why quorum sensing does not always result in truly homogenous cell behavior.* Applied and environmental microbiology, 2015. **81**(16): p. 5280-5289.
9. Campbell, K., J. Vowinckel, and M. Ralser, *Cell-to-cell heterogeneity emerges as consequence of metabolic cooperation in a synthetic yeast community.* Biotechnology journal, 2016. **11**(9): p. 1169.
10. Clarke, D.J., *The genetic basis of the symbiosis between Photorhabdus and its invertebrate hosts*, in *Advances in applied microbiology*. 2014, Elsevier. p. 1-29.
11. Gefen, O. and N.Q. Balaban, *The importance of being persistent: heterogeneity of bacterial populations under antibiotic stress.* FEMS microbiology reviews, 2009. **33**(4): p. 704-717.
12. ThermoFisher Scientific. *Single Cell Analysis*. Available from: https://www.thermofisher.com/no/en/home/life-science/cell-analysis/single-cell-analysis.html.
13. Andersson, H. and A. van den Berg, *Microtechnologies and nanotechnologies for single-cell analysis.* Current opinion in biotechnology, 2004. **15**(1): p. 44-49.
14. Losick, R. and C. Desplan, *Stochasticity and cell fate.* science, 2008. **320**(5872): p. 65-68.

15. Jonczyk, R., et al., *Living cell microarrays: an overview of concepts*. Microarrays, 2016. **5**(2): p. 11.
16. Bailey, S.N., R.Z. Wu, and D.M. Sabatini, *Applications of transfected cell microarrays in high-throughput drug discovery.* Drug discovery today, 2002. **7**(18): p. S113-S118.
17. Théry, M., *Micropatterning as a tool to decipher cell morphogenesis and functions.* J Cell Sci, 2010. **123**(24): p. 4201-4213.
18. Xu, L., et al., *Microcontact printing of living bacteria arrays with cellular resolution.* Nano letters, 2007. **7**(7): p. 2068-2072.
19. Berkowski, K.L., et al., *Introduction to photolithography: Preparation of microscale polymer silhouettes.* Journal of chemical education, 2005. **82**(9): p. 1365.
20. Eveflow. *HOW TO CHOOSE THE RIGHT PHOTOMASK TO FABRICATE YOUR SU-8 MICROFLUIDIC MOLD?* 2018; Available from: https://www.elveflow.com/microfluidic-tutorials/soft-lithography-reviews-and-tutorials/how-to-choose-your-soft-lithography-instruments/su-8-photolithography-photomask/.
21. Quirk, M. and J. Serda, *Semiconductor manufacturing technology*. Vol. 1. 2001: Prentice Hall Upper Saddle River, NJ.
22. Marc J.Madou, *Fundamentals of Microfabrication*. second ed. 2001, United states of America: CRC press. 703.
23. Ruiz, S.A. and C.S. Chen, *Microcontact printing: A tool to pattern.* Soft Matter, 2007. **3**(2): p. 168-177.
24. Khademhosseini, A., et al., *Microscale technologies for tissue engineering and biology.* Proceedings of the National Academy of Sciences of the United States of America, 2006. **103**(8): p. 2480-2487.
25. Kaufmann, T. and B.J. Ravoo, *Stamps, inks and substrates: polymers in microcontact printing.* Polymer Chemistry, 2010. **1**(4): p. 371-387.
26. TrsN, J., X. YoUNRN, and G.M. WHITeSIDES, *Microcontact Printing of SAMs.*
27. Pariani, G., et al., *Adaptable Microcontact Printing via Photochromic Optical-Saturable Lithography.* Advanced Materials Technologies, 2018. **3**(3): p. 1700325.
28. Xia, Y. and G.M. Whitesides, *Soft lithography.* Annual review of materials science, 1998. **28**(1): p. 153-184.
29. Waters, L.J., et al., *Effect of plasma surface treatment of poly (dimethylsiloxane) on the permeation of pharmaceutical compounds.* Journal of Pharmaceutical Analysis, 2017. **7**(5): p. 338-342.

30. Bodas, D. and C. Khan-Malek, *Hydrophilization and hydrophobic recovery of PDMS by oxygen plasma and chemical treatment—An SEM investigation.* Sensors and Actuators B: Chemical, 2007. **123**(1): p. 368-373.
31. Fritz, J.L. and M.J. Owen, *Hydrophobic recovery of plasma-treated polydimethylsiloxane.* The Journal of Adhesion, 1995. **54**(1-4): p. 33-45.
32. Gopal Ashwini, K.H., Xiaojing Zhang,. *Microcontact Printing*. Springerlink, 2017; Available from: https://link.springer.com/referenceworkentry/10.1007/978-90-481-9751-4_337.
33. Shih, T.-K., et al., *Fabrication of PDMS (polydimethylsiloxane) microlens and diffuser using replica molding.* Microelectronic Engineering, 2006. **83**(11-12): p. 2499-2503.
34. Sharp, K.G., et al., *Effect of stamp deformation on the quality of microcontact printing: theory and experiment.* Langmuir, 2004. **20**(15): p. 6430-6438.
35. Tenaillon, O., et al., *The population genetics of commensal Escherichia coli.* Nature Reviews Microbiology, 2010. **8**(3): p. 207.
36. Möckl, L., et al., *En route from artificial to natural: Evaluation of inhibitors of mannose-specific adhesion of E. coli under flow*. Biochimica et Biophysica Acta (BBA)-General Subjects, 2016. **1860**(9): p. 2031-2036.
37. Ofek, I., D. Mirelman, and N. Sharon, *Adherence of Escherichia coli to human mucosal cells mediated by mannose receptors.* Nature, 1977. **265**(5595): p. 623.
38. Sauer, M.M., et al., *Catch-bond mechanism of the bacterial adhesin FimH.* Nature communications, 2016. **7**: p. 10738.
39. Schembri, M.A. and P. Klemm, *Heterobinary Adhesins Based on theEscherichia coli FimH Fimbrial Protein.* Applied and environmental microbiology, 1998. **64**(5): p. 1628-1633.
40. Schembri, M.A., et al., *Molecular characterization of the Escherichia coli FimH adhesin.* The Journal of infectious diseases, 2001. **183**(Supplement_1): p. S28-S31.
41. Pizarro-Cerdá, J. and P. Cossart, *Bacterial adhesion and entry into host cells.* Cell, 2006. **124**(4): p. 715-727.
42. Potthoff, E., et al., *Bacterial adhesion force quantification by fluidic force microscopy.* Nanoscale, 2015. **7**(9): p. 4070-4079.
43. Tester, R.F. and F.H. Al-Ghazzewi, *Mannans and health, with a special focus on glucomannans.* Food Research International, 2013. **50**(1): p. 384-391.

44. Sato, S., et al., *One-pot reductive amination of aldehydes and ketones with α-picoline-borane in methanol, in water, and in neat conditions.* Tetrahedron, 2004. **60**(36): p. 7899-7906.
45. Shima, S. and H. Sakai, *Poly-L-lysine produced by Streptomyces. Part II. Taxonomy and fermentation studies.* Agricultural and Biological Chemistry, 1981. **45**(11): p. 2497-2502.
46. Choi, J.-H., et al., *Influence of pH and surface chemistry on poly (L-lysine) adsorption onto solid supports investigated by quartz crystal microbalance with dissipation monitoring.* The Journal of Physical Chemistry B, 2015. **119**(33): p. 10554-10565.
47. Colville, K., et al., *Effects of poly (L-lysine) substrates on attached Escherichia coli bacteria.* Langmuir, 2009. **26**(4): p. 2639-2644.
48. Methods in Molecular Biology, v., *Microarrays*. second ed, ed. Jang B Rampal. Vol. 1: Synthesis Methods. 2007, Totowa, New Jersey: Humana Press Inc.
49. ThermoFisher Scientific, *Fluorescein (FITC).* 2017.
50. Liebscher, J.r., et al., *Structure of polydopamine: a never-ending story?* Langmuir, 2013. **29**(33): p. 10539-10548.
51. Madhurakkat Perikamana, S.K., et al., *Materials from mussel-inspired chemistry for cell and tissue engineering applications.* Biomacromolecules, 2015. **16**(9): p. 2541-2555.
52. Biotechnical and Biomedical Applications, *Poly(Ethylene Glycol) Chemistry*. First ed. 1992, New York: Plenum Publishing Corporation. 371.
53. Oh, Y., et al., *Micropatterning of bacteria on two-dimensional lattice protein surface observed by atomic force microscopy.* Ultramicroscopy, 2008. **108**(10): p. 1124-1127.
54. Lih, E., et al., *Polymers for cell/tissue anti-adhesion.* Progress in polymer science, 2015. **44**: p. 28-61.
55. Park, K.D., et al., *Bacterial adhesion on PEG modified polyurethane surfaces.* Biomaterials, 1998. **19**(7-9): p. 851-859.
56. Cheng, G., et al., *Inhibition of bacterial adhesion and biofilm formation on zwitterionic surfaces.* Biomaterials, 2007. **28**(29): p. 4192-4199.
57. Stephen Gallik. *Bright-field Microscopy*. 2009; Available from: http://histologyolm.stevegallik.org/node/28.
58. Zeiss and M.W. Davidson. *Basic Microscopy*. Available from: https://www.zeiss.com/microscopy/int/solutions/reference/basic-microscopy/koehler-illumination.html.
59. DOC PLAYER, *MICROSCOPY I: BRIGHT-FIELD.* 2018.

60. Microscope, L.s.S., *Numerical Aperture and Resolution.* 1998 [last modification: 2015].
61. Robert Bagnell, *Phase ContrastC.* 2012.
62. Olympus, et al. *Basic Concepts in Fluorescence*. 2018; Available from: https://www.olympus-lifescience.com/en/microscope-resource/primer/techniques/fluorescence/fluorescenceintro/.
63. Thorn, K., *A quick guide to light microscopy in cell biology.* Molecular biology of the cell, 2016. **27**(2): p. 219-222.
64. ThermoFisher Scientific, *Anatomy of Fluorescence Spectra.* 2018.
65. Chang, K.-C., et al., *Atomic force microscopy in biology and biomedicine.* Tzu Chi Medical Journal, 2012. **24**(4): p. 162-169.
66. Dufrêne, Y.F., et al., *Multiparametric imaging of biological systems by force-distance curve–based AFM.* Nature methods, 2013. **10**(9): p. 847.
67. Fang, H.H., K.-Y. Chan, and L.-C. Xu, *Quantification of bacterial adhesion forces using atomic force microscopy (AFM).* Journal of microbiological methods, 2000. **40**(1): p. 89-97.
68. Dunker, K., *Microarrays for High Throughput Analysis of Cellular Heterogeneity*. 2017, NTNU.
69. Ottesen, V., *Bacterial Microarrays by Microcontact Printing: Development of a Method for Immobilizing Live Bacteria on Microarrays*. 2014, Institutt for fysikk.
70. Whitesides, G.M., *The origins and the future of microfluidics.* Nature, 2006. **442**(7101): p. 368.